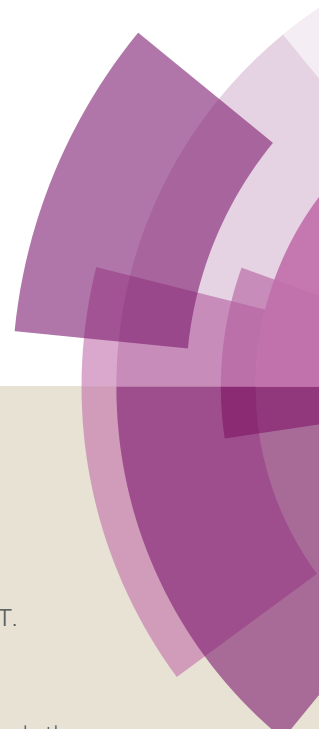
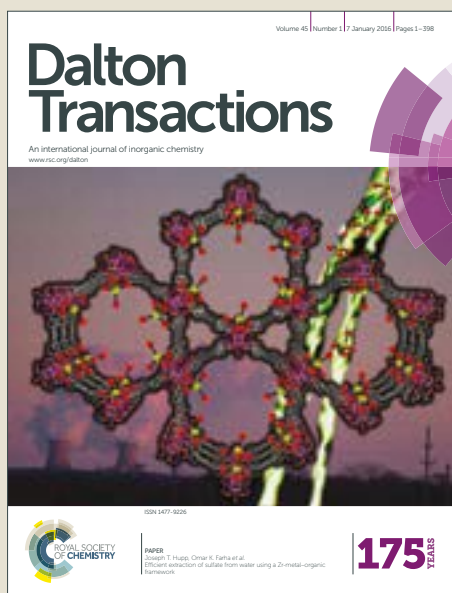


Dalton Transactions

Accepted Manuscript



This article can be cited before page numbers have been issued, to do this please use: M. M. Cetin, R. T. Hodson, C. R. Hart, D. B. Cordes, M. Findlater, D. J. Casadonte, A. F. Cozzolino and M. F. Mayer, *Dalton Trans.*, 2017, DOI: 10.1039/C7DT00400A.



This is an Accepted Manuscript, which has been through the Royal Society of Chemistry peer review process and has been accepted for publication.

Accepted Manuscripts are published online shortly after acceptance, before technical editing, formatting and proof reading. Using this free service, authors can make their results available to the community, in citable form, before we publish the edited article. We will replace this Accepted Manuscript with the edited and formatted Advance Article as soon as it is available.

You can find more information about Accepted Manuscripts in the [author guidelines](#).

Please note that technical editing may introduce minor changes to the text and/or graphics, which may alter content. The journal's standard [Terms & Conditions](#) and the ethical guidelines, outlined in our [author and reviewer resource centre](#), still apply. In no event shall the Royal Society of Chemistry be held responsible for any errors or omissions in this Accepted Manuscript or any consequences arising from the use of any information it contains.



Journal Name

ARTICLE

Synthesis, structural characterization, photophysical properties, DFT and TDDFT calculations, and photoredox catalysis studies of 2,9-di(aryl)-1,10-phenanthroline copper (I) complexes

Received 00th January 20xx,
Accepted 00th January 20xx

DOI: 10.1039/x0xx00000x

www.rsc.org/

M. Mustafa Cetin,^a Roman T. Hodson,^a C. Robin Hart,^a David B. Cordes,^b Michael Findlater,^a Dominick J. Casadonte, Jr.,^a Anthony F. Cozzolino,^a Michael F. Mayer*^a

The synthesis, characterization, photophysical properties, theoretical calculations, and catalytic applications of 2,9-di(aryl)-1,10-phenanthroline copper (I) complexes are described. Specifically, this study made use of di(aryl)-1,10-phenanthroline ligands including 2,9-di(4-methoxyphenyl)-1,10-phenanthroline (**1**), 2,9-di(4-hydroxyphenyl)-1,10-phenanthroline (**2**), 2,9-di(4-methoxy-3-methylphenyl)-1,10-phenanthroline (**3**), and 2,9-di(4-hydroxy-3-methylphenyl)-1,10-phenanthroline (**4**). The 2:1 ligand-to-metal complexes, as PF₆⁻ salts, i.e., [(Cu·(**1**)₂)PF₆], [Cu·(**2**)₂]PF₆, [Cu·(**3**)₂]PF₆, and [Cu·(**4**)₂]PF₆ have been isolated and characterized. The structures of ligands **1** and **2** and complexes [Cu·(**1**)₂]PF₆ and [Cu·(**3**)₂]PF₆ have been determined by single-crystal X-ray analysis. The photoredox catalytic activity of these copper (I) complexes was investigated in an atom-transfer radical addition (ATRA) reaction and the results showed fairly efficient activity, with a strong wavelength dependence. In order to better understand the observed catalytic activity, photophysical emission and absorption studies, and DFT calculations were also performed. It was determined that when the excitation wavelength was appropriate for exciting into the LUMO+1 or LUMO+2, catalysis would occur. On the contrary, excitations into the LUMO resulted in no observable catalysis. In light of these results, a mechanism for the ATRA photoredox catalytic cycle has been proposed.

Introduction

The discovery of 1,10-phenanthroline and its use as a ligand for application in coordination chemistry dates back to the late nineteenth century.¹ Since these early studies, 1,10-phenanthroline and the substituted derivatives have been used extensively for their many desirable structural and chemical properties, such as: aromaticity, basicity, planarity, rigidity, and chelating capability.² As ligands, 1,10-phenanthroline and numerous substituted derivatives strongly coordinate to most of the transition metal ions, in a chelating bidentate fashion, as fairly powerful σ -donors and π -acceptors.^{2a,3} Thus, these ligands and their complexes, e.g., complexes as shown in Fig. 1, have been the subject of a multitude of studies in organic, inorganic and supramolecular chemistry.^{2a,4,5} In particular, there has been much interest in the coordination chemistry, photophysical properties and redox properties of metal-phenanthroline complexes.⁶⁻⁸

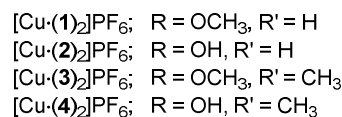
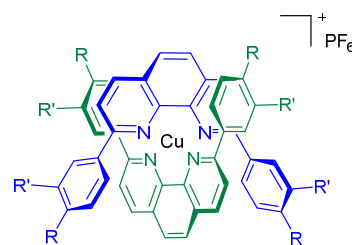


Fig. 1 Structures of [Cu·(**1**)₂]PF₆, [Cu·(**2**)₂]PF₆, [Cu·(**3**)₂]PF₆, [Cu·(**4**)₂]PF₆.

Though the preparation of metal complexes of 1,10-phenanthroline ligands has been studied broadly,¹⁻⁸ the coordination chemistry of substituted 1,10-phenanthroline ligands, in particular, has undergone remarkable growth in recent years.^{2b} Further interest in the complexes has arisen due to their unique structural, magnetic, electronic, and

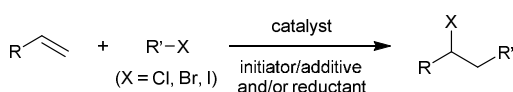
^a Department of Chemistry and Biochemistry, Texas Tech University, MS 41061, Lubbock, TX 79409, USA, Fax: 001 806 742 1289; Tel: 001 806 834 3689; E-mail: mf.mayer@ttu.edu

^b EaStCHEM School of Chemistry, University of St. Andrews, St. Andrews, KY16 9ST, U.K.

spectroscopic properties. These compounds have been used as: luminescent probes,⁷ contrast agents for magnetic resonance imaging (MRI),⁸ components in efficient light-emitting devices,^{9,10} sensitizers for solar hydrogen catalysis,¹¹ and shift reagents for nuclear magnetic resonance (NMR) experiments.¹²

The robust nature of metal-phenanthroline complexes also makes them attractive scaffolds for the development of transition metal-based catalysts. A broad range of transformations are now reported to be catalyzed by metal-phenanthroline complexes, including: Mizoroki-Heck coupling,¹³ alcohol oxidation,¹⁴ conjugate addition,¹⁵ asymmetric catalysis,¹⁶ ethylene oligomerization,¹⁷ metal-promoted C-C coupling,^{3b,18} photoredox catalysis,^{19,20} atom-transfer radical-polymerization (ATRP),²⁰ C-H functionalization²¹ and hydroamidation.²² Within this burgeoning new application of metal-phenanthroline complexes, a unique role for copper has emerged. Importantly, copper (I) is an inexpensive, earth-abundant, and attractive alternative to precious metal ions. For example, a copper-based catalyst has been reported to be capable of ATRP with use of a blue LED.^{20a} Miura and co-workers have reported the construction of biaryl heterocycles in good to moderate yields using [(1,10-phenanthroline)CuF₂] and a base at room temperature.²³ In one remarkable example, the direct oxidation of cyclohexane to cyclohexanone was achieved with selectivity using CuCl₂, 1,10-phenanthroline and 2 equivalents of potassium carbonate at room temperature under air.²⁴

Of relevance to the current catalysis study, *vide infra*, metal complexes of 1,10-phenanthroline ligands have also been used in an atom-transfer radical-addition (ATRA) reaction^{19b,25a}, i.e., the Kharasch addition (Scheme 1). ATRA is a fundamental and versatile reaction in which radical addition of mainly polyhalogenated compounds to a C=C (or C≡C) bond results in the formation of both C-C and C-X bonds. Kharasch and co-workers first reported this addition reaction in 1945 (preliminary studies were carried out in 1937^{25f}).^{25b} Kharasch, in particular, investigated the addition of polyhalogenated methane derivatives, such as CBr₄, CCl₄, CBr₃Cl and CBrCl₃, to olefins in the presence of free radical initiators or light.^{25b,26}



Scheme 1 General atom-transfer radical-addition (ATRA) reaction.

Peroxides,^{25b,27} triethylboron,²⁸ azobisisobutyronitrile (AIBN),²⁹ and organotin reagents³⁰ were commonly used as initiators in ATRA reactions. However, these initiators are not ideal for ATRA reactions due to concerns such as cost, toxicity, air sensitivity, and more importantly, operational safety.^{30c,30e,31} Transition metal (Cu,³² Ru,³³ Fe,³⁴ or Ni³⁵) complexes can be employed as alternatives to these initiators. In order to achieve desirable yields however, these metal complexes are

typically used at relatively high loading. In most of these reactions, ascorbic acid (as a reducing agent), AIBN and V-70 (free-radical initiators and reducing agents for ATRA at ambient temperatures) are used to complete the catalytic cycle by reducing the metal in the complex.²⁵⁻³⁵ As a result of the factors mentioned above, metal-mediated visible light-driven photoredox catalysis with reducing agents has been employed as a useful technique for a growing number of organic transformations.^{2b,36,37}

The use of a relatively low loading of copper catalyst in a few successful ATRA reactions^{19b,30a,38} has encouraged us to further investigate and improve the understanding of these photocatalytic ATRA reactions. In light of these reports, we prepared and probed 2,9-di(aryl)-1,10-phenanthroline copper (I) complexes with various substituents (Fig. 1). More specifically, herein we report the preparation, structural characterization, photophysical properties, theoretical calculations and catalytic studies of complexes [Cu-(**1**)₂]PF₆, [Cu-(**2**)₂]PF₆, [Cu-(**3**)₂]PF₆, and [Cu-(**4**)₂]PF₆. Importantly, the results of these catalytic studies show very efficient catalytic activity, with 100% atom economy, without the use of any reducing agents. All theoretical, synthetic, spectroscopic, photophysical and catalytic results for the copper (I) complexes of 2,9-di(aryl)-1,10-phenanthroline ligands are presented along with X-ray crystal structures of some of the ligands and complexes, i.e., **1**, **2**, [Cu-(**1**)₂]PF₆, and [Cu-(**3**)₂]PF₆.

Experimental

Materials and methods

Anhydrous dichloromethane and acetonitrile were distilled over CaH₂ under nitrogen and stored over molecular sieves prior to use. Ligands (**1** and **2**)³⁹ and ligands (**3** and **4**)⁴⁰ were prepared using known literature procedures. [Cu(CH₃CN)₄]PF₆ was purchased from Aldrich. Styrene was purchased from Acros (stabilized, 99%) and the inhibitor (*p*-tert-butylcatechol) was removed by passing the styrene through a basic alumina column prior to use. All other starting materials were either purchased from commercial sources and used without any further purification, or they were prepared according to the procedures reported in literature. ¹H NMR and ¹³C NMR (decoupled mode) spectra were recorded on a JEOL ECS-400 or Varian Unity Inova 500 MHz spectrometer. DMSO-*d*₆ (99.9% D with 0.05% v/v TMS) was used as the NMR sample solvent.

Preparation of ligands and complexes

The syntheses of the ligands (**1-4**) have been previously reported.^{39,40} The detailed synthetic procedures for the complexes and the molecular structural characterization data for the target compounds are presented below.

[Cu(2,9-(4-MeOC₆H₄)₂-1,10-phen)₂]PF₆ ([Cu-(**1**)₂]PF₆)

A solution of **1** (100 mg, 0.255 mmol) in DCM (10 mL) and acetonitrile (10 mL) was prepared at room temperature under a nitrogen atmosphere. The orange-colored solution was

stirred until ligand **1** was dissolved completely. To this solution, tetrakis(acetonitrile)copper(I) hexafluorophosphate (47.5 mg, 0.127 mmol) was added and the solution was stirred for 20 minutes at room temperature. The color of the solution turned to a dark red-black. Concentration of the mixture under reduced pressure using a rotary evaporator provided the crude product. Purification on silica gel by flash column chromatography, using DCM-methanol (99:1) as eluent, afforded the corresponding copper (I) complex, [Cu-(**1**)₂]PF₆, (107.4 mg, 85%) as a red glassy solid, m.p. >260 °C; ¹H NMR (500 MHz, *d*₆-DMSO) δ 8.69 (d, *J* = 8.5 Hz, 4H), 8.17 (s, 4H), 8.01 (d, *J* = 8.5 Hz, 4H), 7.44 (d, *J* = 8.5 Hz, 8H), 6.05 (d, *J* = 8.5 Hz, 8H), 3.38 (s, 12H); ¹³C NMR (125 MHz, *d*₆-DMSO) δ 159.6, 155.6, 142.8, 137.3, 130.9, 129.1, 127.7, 126.0, 124.2, 112.2, 54.8; HRMS (ESI) *m/z* calcd for C₅₂H₄₀CuN₄O₄ [M-PF₆]⁺ 847.2340, found 847.2346; Anal. calcd for C₅₂H₄₀CuF₆N₄O₄P: C, 62.87; H, 4.06; N, 5.64; found: C, 62.50; H, 3.68; N, 5.82.

[Cu(2,9-(4-HOC₆H₄)₂-1,10-phen)₂]PF₆ ([Cu-(**2**)₂]PF₆)

A solution of **2** (100 mg, 0.274 mmol) in DCM (10 mL) and acetonitrile (10 mL) was prepared at room temperature under a nitrogen atmosphere. The yellow-colored solution was stirred until ligand **2** was dissolved completely. To this solution, tetrakis(acetonitrile)copper(I) hexafluorophosphate (51.1 mg, 0.137 mmol) was added and the solution was stirred for 20 minutes at room temperature. The color of the solution turned to a dark red-black. Concentration of the mixture under reduced pressure using a rotary evaporator provided the crude product. Purification on silica gel by flash column chromatography, using DCM-methanol (99:1) as eluent, afforded the corresponding copper (I) complex, [Cu-(**2**)₂]PF₆, (107.5 mg, 84%) as a red glassy solid, m.p. >260 °C; ¹H NMR (400 MHz, *d*₆-DMSO) δ 9.33 (s, 4H), 8.65 (d, *J* = 8.3 Hz, 4H), 8.14 (s, 4H), 7.95 (d, *J* = 8.2 Hz, 4H), 7.34 (d, *J* = 8.7 Hz, 8H), 5.88 (d, *J* = 8.7 Hz, 8H); ¹³C NMR (100 MHz, *d*₆-DMSO) δ 158.1, 155.8, 142.9, 137.2, 129.4, 129.1, 127.6, 126.0, 124.1, 113.6; HRMS (ESI) *m/z* calcd for C₄₈H₃₂CuN₄O₄ [M-PF₆]⁺ 791.1714, found 791.1698; Anal. calcd for C₄₈H₃₂CuF₆N₄O₄P: C, 61.51; H, 3.44; N, 5.98; found: C, 61.37; H, 3.52; N, 5.59.

[Cu(2,9-(3-Me-4-MeOC₆H₃)₂-1,10-phen)₂]PF₆ ([Cu-(**3**)₂]PF₆)

A solution of **3** (100 mg, 0.238 mmol) in DCM (10 mL) and acetonitrile (10 mL) was prepared at room temperature under a nitrogen atmosphere. The light yellow-colored solution was stirred until ligand **3** was dissolved completely. To this solution, tetrakis(acetonitrile)copper(I) hexafluorophosphate (44.3 mg, 0.119 mmol) was added and the solution was stirred for 20 minutes at room temperature. The color of the solution turned to a dark brown-red-black. Concentration of the mixture under reduced pressure using a rotary evaporator provided the crude product. Purification on silica gel by flash column chromatography, using DCM-methanol (99:1) as eluent, afforded the corresponding copper (I) complex, [Cu-(**3**)₂]PF₆, (106.6 mg, 85%) as a red glassy solid, m.p. >260 °C; ¹H NMR (400 MHz, *d*₆-DMSO) δ 8.67 (d, *J* = 8.7 Hz, 4H), 8.17 (s, 4H), 8.00 (d, *J* = 8.2 Hz, 4H), 7.43 (s, 4H), 7.25 (d, *J* = 8.7 Hz, 4H), 6.27 (d, *J* = 8.2 Hz, 4H), 3.51 (s, 12H), 1.05 (s, 12H); ¹³C

NMR (100 MHz, *d*₆-DMSO) δ 157.8, 155.7, 142.9, 137.0, 130.4, 129.2, 127.5, 126.5, 126.0, 124.0, 124.0 108.7, 55.2, 14.9; HRMS (ESI) *m/z* calcd for C₅₆H₄₈CuN₄O₄ [M-PF₆]⁺ 903.2966, found 903.2939; Anal. calcd for C₅₆H₄₈CuF₆N₄O₄P: C, 64.09; H, 4.61; N, 5.34; found: C, 63.94; H, 4.65; N, 4.94.

[Cu(2,9-(3-Me-4-HOC₆H₃)₂-1,10-phen)₂]PF₆ ([Cu-(**4**)₂]PF₆)

A solution of **4** (100 mg, 0.255 mmol) in DCM (10 mL) and acetonitrile (10 mL) was prepared at room temperature under a nitrogen atmosphere. The dark green-colored solution was stirred until ligand **4** was dissolved completely. To this solution, tetrakis(acetonitrile)copper(I) hexafluorophosphate (47.5 mg, 0.127 mmol) was added and the solution was stirred for 20 minutes at room temperature. The color of the solution turned to a dark red-black. Concentration of the mixture under reduced pressure using a rotary evaporator provided the crude product. Purification on silica gel by flash column chromatography, using DCM-methanol (99:1) as eluent, afforded the corresponding copper (I) complex, [Cu-(**4**)₂]PF₆, (106.7 mg, 84%) as a red glassy solid, m.p. >260 °C; ¹H NMR (500 MHz, *d*₆-DMSO) δ 9.30 (s, 4H), 8.61 (d, *J* = 8.5 Hz, 4H), 8.14 (s, 4H), 7.91 (d, *J* = 8.5 Hz, 4H), 7.45 (s, 4H), 7.08 (dd, *J* = 2.0, 8.0 Hz, 4H), 6.23 (d, *J* = 8.5 Hz, 4H), 0.84 (s, 12H); ¹³C NMR (125 MHz, *d*₆-DMSO) δ 156.3, 155.8, 142.9, 136.8, 129.5, 129.2, 127.4, 125.9, 124.0, 122.2, 113.0, 49.0, 14.6; HRMS (ESI) *m/z* calcd for C₅₂H₄₀CuN₄O₄ [M-PF₆]⁺ 847.2340, found 847.2348; Anal. calcd for C₅₂H₄₀CuF₆N₄O₄P: C, 62.87; H, 4.06; N, 5.64; found: C, 62.49; H, 3.87; N, 5.52.

General procedure of photoredox ATRA reaction to provide (1,3,3,3-tetrabromopropyl)benzene

The protocol for this photoredox reaction was adapted from a literature report.^{19b} A solution of styrene (1.5 mmol), carbon tetrabromide (1.5 mmol), and copper (I) complex ([Cu-(**1**)₂]PF₆–[Cu-(**4**)₂]PF₆) (0.3 mol%) in 1.5 mL CH₂Cl₂ was placed under an argon atmosphere in a capped 20 mL vial equipped with a magnetic stirring bar. Then the dark red-colored reaction mixture was stirred and irradiated with an LED light (Figs. S9 and S10) for 20 hours at room temperature. (Another set of reactions involved irradiation of the sample with a General Electric 40 W soft white light bulb (Fig. S14) under the, otherwise, same conditions.) After stirring 20 hours, the reaction mixture was concentrated under reduced pressure using a rotary evaporator, washed with brine, and then purified on a short pad of silica gel by elution with pure hexanes.

Crystallography

Diffraction data for compounds [Cu-(**1**)₂]PF₆, [Cu-(**3**)₂]PF₆, and **2**, were obtained on a Bruker Smart Apex II CCD diffractometer, and data for compound **1** were obtained on a Rigaku SCX-Mini CCD diffractometer. Data for compound **2** were collected at room temperature, while those data for compounds [Cu-(**1**)₂]PF₆, [Cu-(**3**)₂]PF₆ and **1** were collected at low temperature ([Cu-(**1**)₂]PF₆ and [Cu-(**3**)₂]PF₆ at 100 K, **1** at 173 K), using graphite-monochromated Mo-Kα radiation (λ =

ARTICLE

Journal Name

0.71073 Å). Intensity data were collected using ω -steps accumulating area detector images spanning at least a hemisphere of reciprocal space. All data were corrected for Lorentz polarization effects. A multi-scan absorption correction was applied using SADABS⁴¹ (compounds [Cu-(**1**)₂]PF₆, [Cu-(**3**)₂]PF₆ and **2**), or CrystalClear⁴² (compound **1**). Structures were solved by direct methods using XS (compounds **1** and **2**) or XM (compounds [Cu-(**1**)₂]PF₆ and [Cu-(**3**)₂]PF₆) and refined by full-matrix least-squares against F^2 (XL). Structure solution and refinement were conducted within the SHELXTL interface.⁴³ All hydrogen atoms bound to carbon were assigned riding isotropic displacement parameters and constrained to idealized geometries. Hydrogen atoms bound to oxygen were located from the difference Fourier map and refined isotropically subject to a distance restraint. Compound [Cu-(**1**)₂]PF₆ was affected by non-merohedral twinning, with a twin law of [0.045 -0.955 -0.056 -1.045 -0.045 0.056 0 0 -1], and a refined twin fraction of 0.34. This was accounted for in the refinement by the use of an HKLF5 file, generated using the TWINROT routine in PLATON.⁴⁴ The MeCN solvent molecule in [Cu-(**3**)₂]PF₆ showed symmetry-induced disorder by reflection. Compound **1** appeared to contain diffuse, disordered solvent molecules running along the *c*-axis, which could not be adequately modelled. The SQUEEZE procedure in PLATON was used to remove the electronic contribution from this solvent, amounting to 138 electrons per unit cell, or 23 electrons per molecule. This was taken to be equivalent to two waters per molecule of **1**. The electron density thus accounted for has been included in the formula, formula weight, ρ , μ and $F(000)$. Crystal and refinement details are summarized in Table S6.

Photophysical measurements

Absorption spectra were obtained using a Shimadzu UV-2401PC, UV-VIS recording spectrophotometer. The emission spectra were obtained using an SLM 8000 fluorimeter that was retrofitted for single photon counting by the Ollis Corporation. Lifetime measurements were obtained on a Jobin Yvon HR time-correlated single-photon counting (TCSPC) spectrometer. All lifetime measurements were obtained in triplicate. The Cu(I) solutions were prepared in dried DCM under argon in an LC technologies LC-1 glovebox.

Calculations

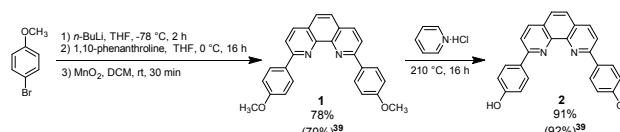
Calculations were performed using the ORCA 3.0 quantum chemistry program package from the development team at the Max Planck Institute for Bioinorganic Chemistry.⁴⁵ For geometry optimizations the LDA and GGA functionals employed were those of Perdew and Wang (PW-LDA, PW91).⁴⁶ All geometry optimizations were carried out using the def2-TZV(2pf) basis set for the copper atoms, the def2-TZV basis set for the hydrogen atoms, and the def2-TZV(p) set for all others.^{47,48} Spin-restricted Kohn–Sham determinants were chosen to describe the closed shell wavefunctions, employing the RI approximation⁴⁹ and the tight SCF convergence criteria provided by ORCA. All geometry optimizations were followed

by frequency calculations using the analytical frequencies option in ORCA to ensure that there are no negative frequencies. TDDFT was used to calculate the 50 and 200 lowest energy singlet and triplet excitations for the ligands and complexes, respectively with PW91 to establish the general ordering of transitions. Additional polarization functions were added to the H and main-group elements for the TDDFT calculations. TDDFT calculations were also run with the hybrid functionals using Becke (B88)⁵⁰ with 30% HF for the exchange and Perdew and Wang (PW91)⁴⁶ for the correlation on the lowest 10 transitions for the ligand and the lowest 20 transitions for the complex.

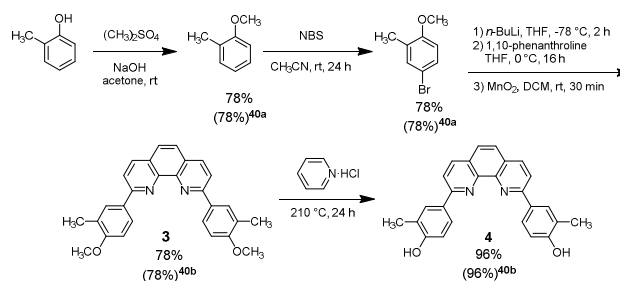
Results and Discussion

Synthesis of ligands 1-4

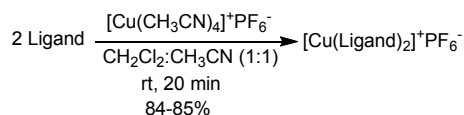
Ligands **1-4** were synthesized (Schemes 2 and 3) in high yield by use of literature procedures.^{39,40} The ligands were characterized by spectroscopic analysis and the spectra matched that reported in the literature.^{39,40} In this work, the solid-state structures of ligands **1** and **2** were determined by single-crystal x-ray analysis.

Scheme 2 Synthesis of ligands **1** and **2**.

The two methyl groups directly bonded to the phenyl rings, in both ligands **3** and **4**, helped serve as additional spectroscopic markers for identification of the ligands as well as the corresponding copper (I) complexes of **3** and **4**.

Scheme 3 Synthesis of ligands **3** and **4**.Synthesis of copper (I) complexes [Cu-(**1**)₂]PF₆-[Cu-(**4**)₂]PF₆

Bis(2,9-di(aryl)-1,10-phenanthroline) copper (I) complexes [Cu-(**1**)₂]PF₆-[Cu-(**4**)₂]PF₆ were synthesized in high yield, as shown in Scheme 4, and they were characterized by a variety of spectroscopic techniques. The complexes are air-stable and capable of being dissolved in most common organic solvents. The solid-state structures of two of the complexes ([Cu-(**1**)₂]PF₆ and [Cu-(**3**)₂]PF₆) were determined by single-crystal x-ray analysis.



Scheme 4 General synthetic scheme for the synthesis of complexes.

X-ray structures of ligands 1 and 2

Colorless and yellow single crystals of ligands **1** and **2** were grown by slow cooling and evaporation of the ethanol and ethanol/water (1:1), solutions, respectively. Both of these compounds adopt slight variations on what might be the expected geometry of the compound, with the phenanthroline adopting an almost planar arrangement in both compounds, and the benzene rings twisted out of the plane by varying amounts (Fig. 2).

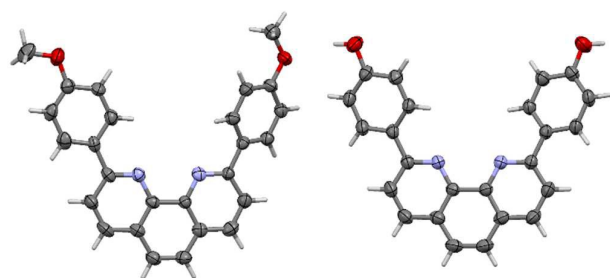


Fig. 2 Structure of ligand **1** (left) and ligand **2** (right, water molecules have been omitted for clarity). Thermal ellipsoids are drawn at the 50% probability level.

Ligand **1** shows slightly less planarity in the phenanthroline than **2** (RMS deviations from planarity are 0.0065 and 0.0631 Å, respectively), with the benzene rings twisted out of this plane by 26.59(6)° for **2**, compared with 5.2(2)° and 28.4(3)° for **1**. Despite the apparent physical similarities between **1** and **2**, the intermolecular interactions seen in their X-ray structures vary greatly. In compound **1**, the primary intermolecular interactions are a series of CH/π interactions, between aryl hydrogens and the methoxyphenyl rings of the compound [C–H⋯centroid distances 2.70–2.86 Å, C⋯centroid distances 3.447(7)–3.763(7) Å, shortest C–H⋯C distances 2.74–2.86 Å]. These weak interactions, acting together, are the only directional interactions acting in the structure of **1**, as neither π⋯π interactions (shortest distance between centroids 4.62 Å), nor hydrogen-bonds of any type (none observed during early attempts at modelling the disordered water molecules) are seen. In contrast, in compound **2**, no π-interactions of any kind occur (shortest distance between centroids 4.14 Å), two sets of hydrogen bonds comprise the intramolecular interactions. The first set of these, two complementary interactions between the alcohol hydroxy groups and waters [distances: RO–H⋯OH₂ 1.671(17) Å, RO⋯OH₂ 2.6385(18) Å; HO–H⋯OR 1.978(18) Å, HO–H⋯OR 2.8262(19) Å], gives rise to a hydrogen-bonded tetramer of two alcohols and two waters. This tetrameric linker leads to the formation of one-dimensional undulating chains of **2**, running along the [2 0 1] diagonal axis (Fig. 3). The second set of hydrogen bonds,

between one water, and the nitrogen of the phenanthroline [distances: HO–H⋯N 2.00(2) Å, HO⋯N 2.8885(18) Å], and complimented by a weak hydrogen bond between a phenanthroline hydrogen and the same water oxygen anions [distances: CH⋯O 2.60, C⋯O 3.525(2)], links the one-dimensional chains into a three-dimensional network.

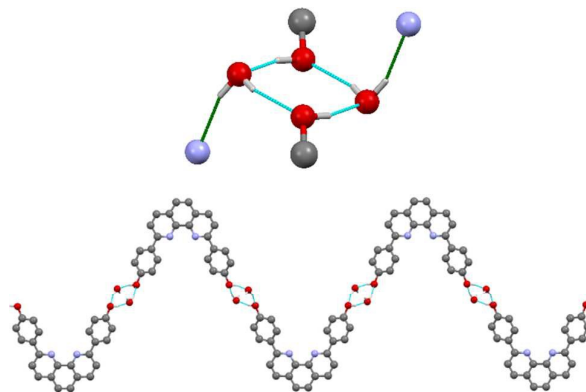


Fig. 3 (bottom) View of the one-dimensional hydrogen bonded chain formed by **2**, propagating along the crystallographic [2 0 1] diagonal axis. Hydrogens, other than those involved in hydrogen-bonding are omitted for clarity. (top) View of the hydrogen-bonded tetrameric linker in **2**. Hydrogen bonds involved in forming the tetranuclear cluster are shown in blue, those further linking adjacent hydrogen-bonded nitrogen atoms are shown in green.

X-ray structures of complexes: [Cu-(**1**)₂]PF₆ and [Cu-(**3**)₂]PF₆

Dark red single crystals of both complexes [Cu-(**1**)₂]PF₆ and [Cu-(**3**)₂]PF₆ were grown by slow cooling and evaporation of a toluene/acetonitrile (1:2) solution. The solid-state structures of each of these complexes (Fig. 4), occupying the triclinic space group *P*1̄ ([Cu-(**1**)₂]PF₆) and the monoclinic space group *C*2/*c* ([Cu-(**3**)₂]PF₆), both comprise two molecules of their respective ligands (**1** and **3**) as well as a PF₆[−] anion. In addition, [Cu-(**3**)₂]PF₆ includes an acetonitrile solvent molecule. The Cu–N bond lengths are all typical [2.026(4) to 2.050(4) Å for [Cu-(**1**)₂]PF₆, 2.049(2) and 2.050(2) Å for [Cu-(**3**)₂]PF₆] of such complexes, and, although the geometries around the Cu atom show significant distortion from the ideal tetrahedral geometry [NCuN/NCuN interplanar angle 71.6° for [Cu-(**1**)₂]PF₆, 72.0° for [Cu-(**3**)₂]PF₆], this is in agreement with previously reported examples.⁵¹ These distortions have been thought to enable a more spatially-efficient packing of the individual complexes.⁵¹

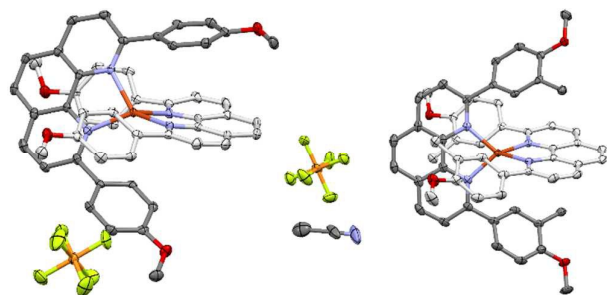


Fig. 4 X-ray structure of the complexes $[\text{Cu}-(1)_2]\text{PF}_6$ (left) and $[\text{Cu}-(3)_2]\text{PF}_6$ with MeCN (right). The backbone atoms of one ligand in each complex have been highlighted to better show the molecular arrangement. Thermal ellipsoids are drawn at the 50% probability level and hydrogens have been omitted for clarity.

This appears to be borne out in $[\text{Cu}-(1)_2]\text{PF}_6$, as this geometry about the metal allows several intramolecular $\pi\cdots\pi$ interactions to take place [centroid \cdots centroid distances 3.643(3) to 3.824(3) Å]. Conversely, in $[\text{Cu}-(3)_2]\text{PF}_6$, only one intramolecular interaction occurred; a very weak C(methyl)H $\cdots\pi$ (phenanthroline) interaction [C–H \cdots centroid distance 3.00 Å, shortest C–H \cdots C distance 2.97 Å]. This distance is slightly larger than the conventional van der Waals limit but CH $\cdots\pi$ interactions have been suggested to be effective at distances beyond this value.^{52,53} In addition, both compounds do show a variety of intermolecular interactions. In $[\text{Cu}-(1)_2]\text{PF}_6$, the more common of these are weak hydrogen bonds between both aromatic and methyl hydrogens and either methoxy oxygens, or fluorides of the PF_6^- anions [CH \cdots acceptor distances 2.24 to 2.59 Å, C \cdots acceptor distances 3.013(8) to 3.383(7)]. Less common are CH/ π interactions between two aryl hydrogens and methoxyphenyl rings [C–H \cdots centroid distances 2.73 and 2.83 Å, C \cdots centroid distances 3.356(6) and 3.457(6) Å, shortest C–H \cdots C distances 2.87 and 2.79 Å]. In $[\text{Cu}-(3)_2]\text{PF}_6$, weak hydrogen bonds are the more common intermolecular interaction, between both aromatic hydrogens of the complex and either nitrogens of the MeCN or fluorides of the PF_6^- anions, as well as between hydrogens of the MeCN and fluorides of the PF_6^- anions [CH \cdots acceptor distances 2.47 to 2.56 Å, C \cdots acceptor distances 3.152(4) to 3.474(8)]. One set of intermolecular $\pi\cdots\pi$ interactions was also found to occur [centroid \cdots centroid distance 3.667(2) Å].

The methyl groups of the 3-methyl-4-methoxyphenyl groups of **3** in complex $[\text{Cu}-(3)_2]\text{PF}_6$ show a *trans* orientation with respect to each other (Fig. 5). The phenyl rings they are bound to are rotated such that, for each ligand, one methyl is positioned above, the other below the plane of the phenanthroline, and the $\text{C}_{\text{phenyl}}-\text{C}_{\text{methyl}}$ bonds are approximately orthogonal to each other.

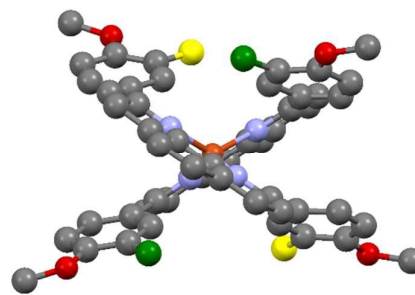


Fig. 5 View of complex $[\text{Cu}-(3)_2]\text{PF}_6$ illustrating the *trans* orientation of methyl groups of each ligand within the complex. The relevant methyl groups are highlighted in green for one ligand, yellow for the other.

NMR spectra of ligands and complexes

The structures of ligands **1-4** (with labelled protons) and the structures of complexes $[\text{Cu}-(1)_2]\text{PF}_6$ – $[\text{Cu}-(4)_2]\text{PF}_6$ are shown in Fig. 6. The ^1H NMR spectra of the ligands and complexes are shown in Fig. 7.

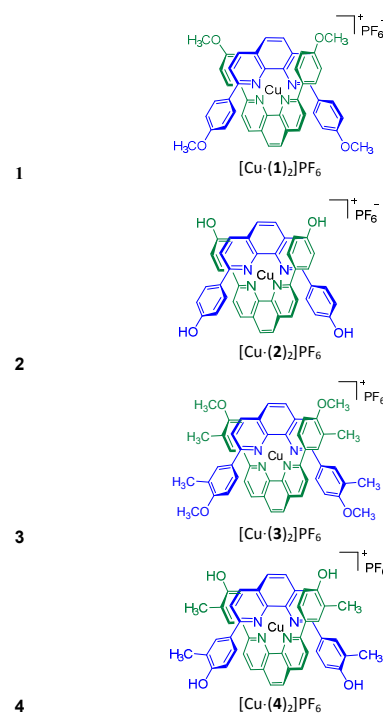


Fig. 6 Structures of **1**, $[\text{Cu}-(1)_2]\text{PF}_6$, **2**, $[\text{Cu}-(2)_2]\text{PF}_6$, **3**, $[\text{Cu}-(3)_2]\text{PF}_6$, **4** and $[\text{Cu}-(4)_2]\text{PF}_6$ with proton labels.

The ^1H NMR spectrum of ligand **1** (Fig. 7a in blue) consisted of just six signals in total (due to both free rotation about the sigma bond that connects the phenyl and phenanthroline moieties as well as average C_{2v} symmetry for the ligand), where there were five signals in the aromatic region and one signal at ca. 3.9 ppm. These signals are assigned to proton sets $\text{H}_a - \text{H}_e$ and OCH_3 , respectively, as labeled in Fig. 6. The ^1H NMR spectrum of $[\text{Cu}-(1)_2]\text{PF}_6$ (Figs. 7a in red) also contained just six signals (due to average D_{2d} symmetry for the complex). In

comparison of the ^1H NMR spectra of **1** and $[\text{Cu}(\cdot\mathbf{1})_2]\text{PF}_6$ (Fig. 7a), all six signals shifted (also see Table S1). Most significantly, the signals for the H_d and H_e proton sets both underwent substantial upfield chemical shifts ($\Delta\delta_{\text{H}_d} = 1.04$ ppm; $\Delta\delta_{\text{H}_e} = 1.13$ ppm), as expected, upon complex formation as a result of the proximity of the H_d and H_e proton sets to the faces of the large aromatic phenanthroline moieties. Such shifts, resulting from a diamagnetic anisotropic effect, are well-documented and they are indicative of bis(2,9-di(aryl)-1,10-phenanthroline) copper (I) complex formation.^{39,40b} Similar shifts were observed in the ^1H NMR spectra of ligand **2** and the corresponding complex $[\text{Cu}(\cdot\mathbf{2})_2]\text{PF}_6$ (Fig. 7b and Table S2).

Comparison of the ^1H NMR spectra of ligand **3** versus $[\text{Cu}(\cdot\mathbf{3})_2]\text{PF}_6$ (as well as ligand **4** versus $[\text{Cu}(\cdot\mathbf{4})_2]\text{PF}_6$) also showed similar diagnostic shifts upon complex formation, Figs. 7c-d and Tables S3 and S4. For ligand **3**, the 6 chemical shift-equivalent methoxy protons produced one singlet at 3.91 ppm, whereas the 6 equivalent methyl protons produced one singlet at 2.35 ppm (Fig. 7c in blue); both signals displayed shifts, intensities and multiplicities in accord with expectations for these common aromatic substituents. For $[\text{Cu}(\cdot\mathbf{3})_2]\text{PF}_6$, while the 12 methoxy protons produced one singlet with a small upfield shift ($\Delta\delta_{\text{OCH}_3} = 0.40$ ppm, compared to **3**), the 12 methyl protons produced one singlet with a very substantial upfield chemical shift ($\Delta\delta_{\text{CH}_3} = 1.30$ ppm, compared to **3**), analogous to the upfield shift observed, upon complexation, for the H_e protons of ligand **1**. This pronounced upfield shift for the protons of the methyl groups in complex $[\text{Cu}(\cdot\mathbf{3})_2]\text{PF}_6$ is a direct manifestation of strong ligand complexation in solution. Ligand **4** and the corresponding complex $[\text{Cu}(\cdot\mathbf{4})_2]\text{PF}_6$ showed a similar large upfield shift ($\Delta\delta_{\text{CH}_3} = 1.47$ ppm).

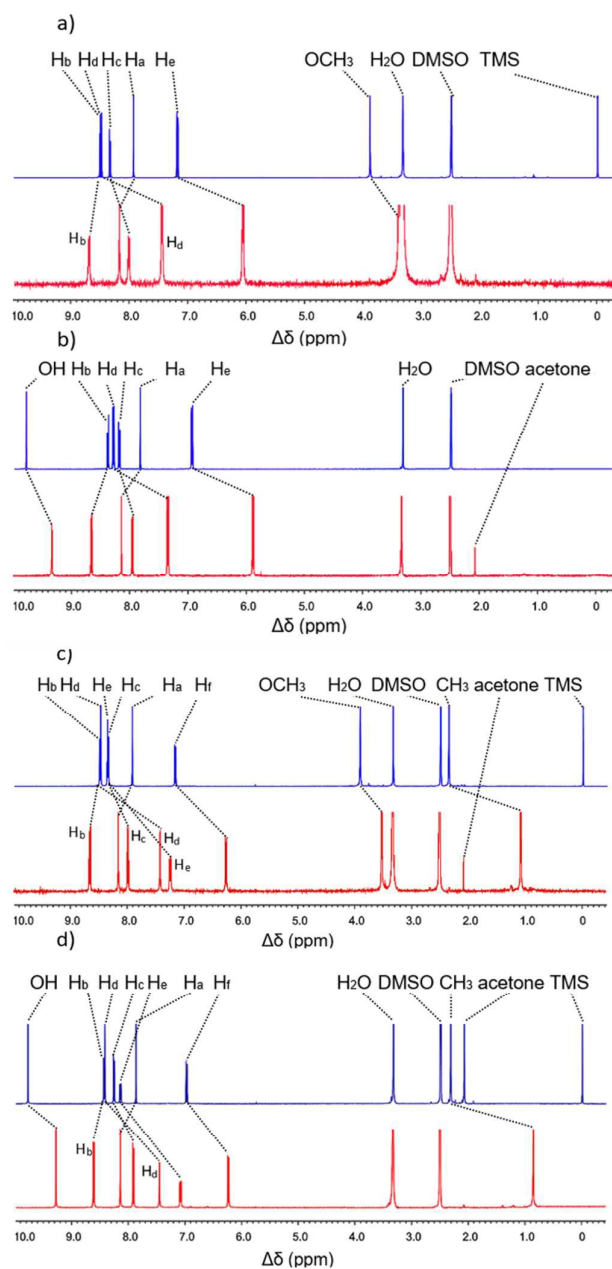


Fig. 7 ^1H NMR spectra of: a) **1** (blue) and $[\text{Cu}(\cdot\mathbf{1})_2]\text{PF}_6$ (red), b) **2** (blue) and $[\text{Cu}(\cdot\mathbf{2})_2]\text{PF}_6$ (red), c) **3** (blue) and $[\text{Cu}(\cdot\mathbf{3})_2]\text{PF}_6$ (red), d) **4** (blue) and $[\text{Cu}(\cdot\mathbf{4})_2]\text{PF}_6$ (red).

Stereoisomers of $[\text{Cu}(\cdot\mathbf{3})_2]\text{PF}_6$ and $[\text{Cu}(\cdot\mathbf{4})_2]\text{PF}_6$, mechanism of cis-trans isomerization

The presence of the methyl groups in ligands **3** and **4**, in contrast to ligands **1** and **2**, allows for numerous limiting stereoisomeric structures for $[\text{Cu}(\cdot\mathbf{3})_2]\text{PF}_6$ and $[\text{Cu}(\cdot\mathbf{4})_2]\text{PF}_6$, respectively. For example, for $[\text{Cu}(\cdot\mathbf{3})_2]\text{PF}_6$, as illustrated in Fig. 6, the two methyl groups of the blue ligand are oriented in opposite (trans) directions; likewise, the two methyl groups of the green ligand are oriented in opposite directions. Thus, Fig. 6 illustrates a trans, trans-isomer (i.e., an atropisomer) of

$[\text{Cu}(\mathbf{3})_2]\text{PF}_6$. The x-ray crystal structure of $[\text{Cu}(\mathbf{3})_2]\text{PF}_6$, as partially shown in Fig. 5, reveals, indeed, a solid-state preference for a pair of enantiomeric trans, trans-atropisomers, again where only one of the two enantiomers present in the crystallographic space group are displayed in Fig. 5. As it is, Fig. 5 and Fig. 6 illustrate the same trans, trans-atropisomer. Again however, also possible are: cis, trans-atropisomers and cis, cis-atropisomers. From molecular models (see Fig. S11 for representations), the cis, cis-atropisomer is chiral and, as such, can exist in two limiting mirror-image forms. The cis, trans-atropisomer is also chiral and can exist in two limiting mirror-image forms. Interestingly, the trans, trans-atropisomer can exist in three separate limiting stereoisomeric forms where two trans, trans-atropisomers are chiral and are mirror-images of one another (as seen in the solid-state) and a third trans, trans-atropisomer is achiral. Thus, in all, seven limiting stereoisomers are possible and, due to degeneracy, four energetically-distinct diastereomeric structures result, i.e., three racemic pairs of enantiomers and one achiral diastereomer.

The ^1H NMR spectrum of $[\text{Cu}(\mathbf{3})_2]\text{PF}_6$ (d_6 -DMSO solution at room temperature) shows just one signal for the 12 protons of the 4 methyl groups (Fig. 7c in red). In principle, such an observation could be consistent with up to three structural/dynamics possibilities. The first possibility, assuming diastereomers to be ^1H NMR-differentiable, is that only one of the racemic pairs of enantiomers (or the achiral diastereomer) of $[\text{Cu}(\mathbf{3})_2]\text{PF}_6$ is present in solution. While such a possibility is consistent with the x-ray structure for $[\text{Cu}(\mathbf{3})_2]\text{PF}_6$, where the solid-state structure was found to be composed of one pair of trans, trans-enantiomers, in this case, this first possibility is unlikely as no particular diastereomer stands out as being more (or less) stable than the others (of the four energetically-distinct diastereomers). The second possibility is that two or more stereoisomers are present but that, by coincidence, there is negligible chemical shift difference for all of the corresponding signals for the various isomers. This second possibility is also unlikely as NMR spectra of $[\text{Cu}(\mathbf{3})_2]\text{PF}_6$ at different ^1H NMR frequencies or in different NMR sample solvents or at different NMR sample temperatures showed no additional signals or even signal broadening for the signal due to the methyl protons. The third possibility is that two or more stereoisomers are present, but where they are in very fast dynamic equilibrium such that the NMR spectrum shows only one signal for the methyl groups with a weighted-average chemical shift.

That no signal broadening was observed in spectra of the complexes, for samples cooled as low as -94°C , suggests that the energetic barrier to cis-trans isomerism is negligible at room temperature for rotation about the sigma bond that connects the phenyl and phenanthroline moieties. Fig. 8 supports this low-energetic-barrier hypothesis as it illustrates a facile mechanism for cis-trans isomerization. In particular, Fig. 8 shows that both planes of the phenyl groups of one ligand of $\mathbf{3}$, in the $[\text{Cu}(\mathbf{3})_2]\text{PF}_6$ complex, are angled outwards and away

(by 30° in the idealized structure) from the sandwiched plane of the phenanthroline moiety of the other ligand in the complex. Due to this angle, it is conceivable that the phenyl groups might be able to rotate 180° such that the methyl group swings between the phenyl and phenanthroline moieties. In contrast, however, it is much more likely that the phenyl group would rotate in the opposite direction. In this direction, a facile cis-trans isomerization can occur where the phenyl group rotates 180° such that the methyl group swings around the outside of the complex (rather than in between the phenyl group and the phenanthroline moieties). Given such a facile mechanism for cis-trans isomerization (i.e., atropisomer interconversion), the average structure in solution is likely within a range of structures on the cis, cis-, cis, trans-, and trans, trans- continuum of stereoisomers (in contrast to the solid-state structural preference for the racemic trans, trans-atropisomers).

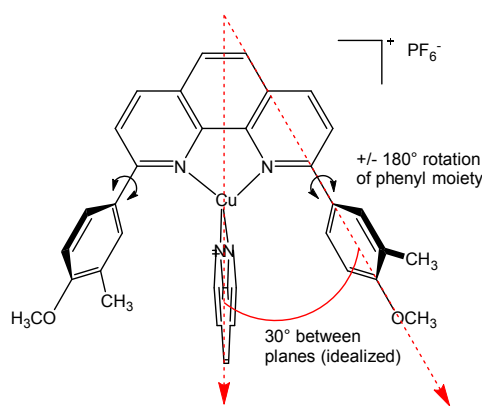


Fig. 8 Mechanism of trans-cis isomerization. A 180° rotation of the shown phenyl groups interconverts the methyl groups on the ligand from a trans to a cis orientation. The phenyl groups of the lower phenanthroline ligand are omitted for clarity.

Absorption studies

The absorption properties of the substituted 1,10-phenanthroline ligands (**1-4**) and the Cu(I) complexes in solution are shown in Fig. 9 and Table 1.

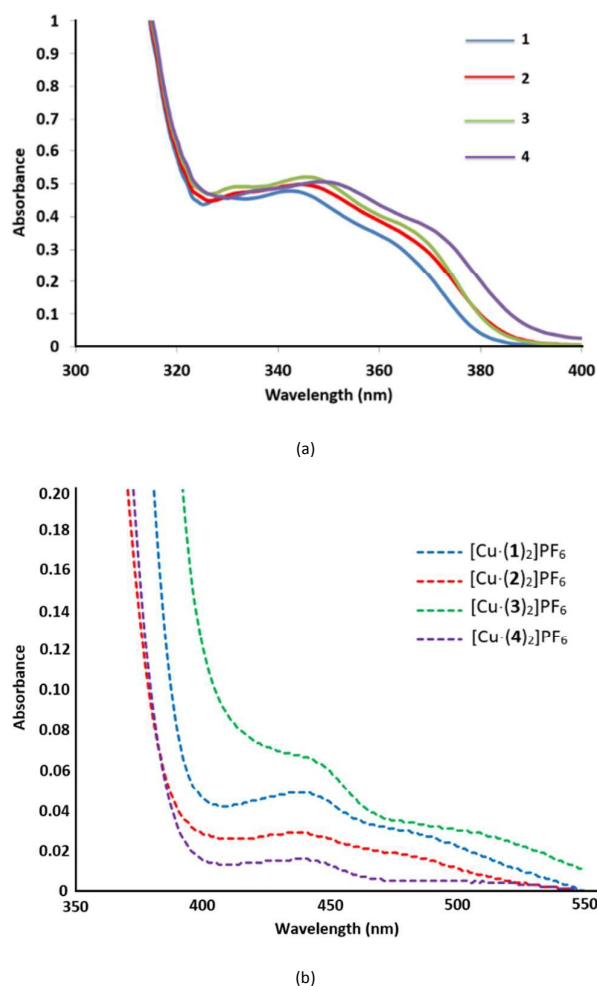


Fig. 9 Absorption spectra of (a) free ligands (in DMSO) and (b) Cu(I) complexes (in DCM).

Table 1 Absorption properties of 1–4 and [Cu-(1)₂]PF₆–[Cu-(4)₂]PF₆

Ligand/Complex	Principal λ_{abs} Max (nm)	(ϵ [$\text{M}^{-1}\text{cm}^{-1}$])	Assignment
1 ^a	286	(7.59×10^4)	¹ L _a
1 ^a	342	(3.57×10^4)	¹ L _b
2 ^a	289	(5.56×10^4)	¹ L _a
2 ^a	345	(2.54×10^4)	¹ L _b
3 ^a	288	(1.47×10^5)	¹ L _a
3 ^a	346	(6.98×10^4)	¹ L _b
4 ^a	289	(1.03×10^5)	¹ L _a
4 ^a	349	(4.95×10^4)	¹ L _b
[Cu-(1) ₂]PF ₆ ^b	440	(4.09×10^3)	¹ MLCT
[Cu-(2) ₂]PF ₆ ^b	438	(3.58×10^3)	¹ MLCT
[Cu-(3) ₂]PF ₆ ^b	442	(7.38×10^3)	¹ MLCT
[Cu-(4) ₂]PF ₆ ^b	439	(8.00×10^3)	¹ MLCT

^aIn dimethyl sulfoxide. ^bIn DCM.

Since ligands 2 and 4 were sparingly soluble in DCM yet fairly soluble in DMSO, DMSO was used as the solvent for all of the photophysical studies of the free ligands. The ligands themselves exhibit ¹ π - π^* absorption bands in dimethyl

sulfoxide (DMSO) solution. However, due to the solvent cut-off window for DMSO (<268 nm), the higher-energy bands typically observed with phenanthrolines in the 220–260 nm region could not be resolved. The free ligands display a band around 286–289 nm and a second, lower-intensity band set between 340 and 350 nm. The peak around 290 nm is most likely the ¹L_a transition (according to the nomenclature of Platt⁵⁴ and Bray⁵⁵). The corresponding transition in unsubstituted 1,10-phenanthroline is also at 289 nm.⁵⁶ This transition is polarized along the long axis (perpendicular to the symmetry axis in each case).^{56,57} The bands between 340 and 350 nm correspond to the lowest-energy ¹ π - π^* transition of the substituted 1,10-phenanthroline ligands (most likely the ¹L_b transition^{54,55}), with a possible admixture of states from the ¹ π - π^* transition of the phenyl substituent. A bathochromic shift of the low-energy absorption bands is typically observed in substituted 1,10-phenanthroline ligands.^{58,59} This has been ascribed in solution to dipole-dipole and induced dipole-dipole interactions in the ground state with a consequent weakening of the ability of the heteroatoms to hydrogen bond (i.e., poorer ground state solvation).^{2e} Another effect which aids in the bathochromic shift of the substituted phenanthrolines is the ability of the phenyl substituents to resonance stabilize the π^* orbitals of the phenanthroline through hyperconjugation. This situation is enhanced by the presence of electron-donating hydroxy and methoxy groups on the phenyl rings.

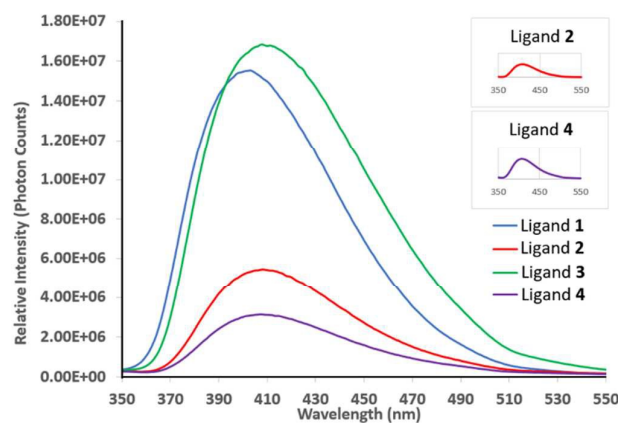
In the visible region, the Cu(I) complexes display the characteristically broad d- π^* metal-to-ligand charge transfer (MLCT) band between 430–470 nm in DCM ($\epsilon = 3.58 \times 10^3 - 8.00 \times 10^3 \text{ M}^{-1}\text{cm}^{-1}$; the peak maxima are listed in Table 1). The blue shift in the charge transfer bands, compared to the Cu(I) 2,9-dimethyl-1,10-phenanthroline analog (454 nm),^{2e} is most likely due to the electron-donating effects of the hydroxy and methoxy groups on the phenyl rings. The reduction in the molar absorptivity of some 2,9-diphenyl-substituted 1,10-phenanthroline Cu(I) complexes has been previously attributed, from a valence bond perspective, to a decrease in the transition dipole length.⁶⁰ The bands of the four copper complexes are broad, unlike the characteristically well-defined peak at 454 nm associated with the 2,9-dimethyl Cu(I) analog.^{2e} This has been suggested by McMillin and Sauvage, in the case of the diphenyl analog, as being due to the low symmetry of the structure in solution for the PF₆⁻ salt.⁶¹

Emission studies

The emission maxima and luminescent lifetimes observed in this study for all of the free ligands and Cu(I) complexes in solution are summarized in Table 2, as are the emission maxima in the solid state. All of the free ligand emission spectra were obtained with DMSO solutions that were absorbance matched to 0.08 ± 0.002 . When the free ligands were excited into the ¹L_b (¹ π - π^*) absorption bands (in DMSO), fluorescence from the ¹ π - π^* states of the phenanthroline ligands was observed, as shown in Fig. 10.

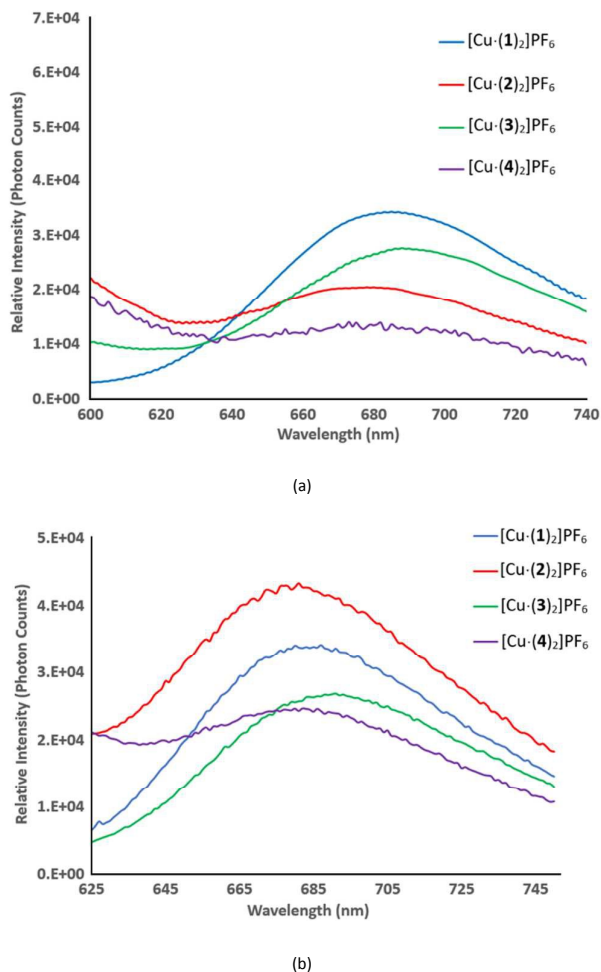
Table 2 Emission data for ligands 1-4 and [Cu-(1)₂]₂PF₆·[Cu-(4)₂]₂PF₆ complexes

Ligand/Complex	Excitation (nm)	Emission Max (nm) ^d and Assignment	Lifetime (ns)
1 ^a	345	405 (¹ L _b (π-π*) emission)	2.6 ± 0.03
2 ^a	345	409 (¹ L _b (π-π*) emission)	2.4 ± 0.07
3 ^a	345	408 (¹ L _b (π-π*) emission)	2.9 ± 0.02
4 ^a	345	407 (¹ L _b (π-π*) emission)	2.9 ± 0.03
[[Cu-(1) ₂] ₂ PF ₆] ^b	467	685 (principal MLCT emission)	236 ± 2
[[Cu-(2) ₂] ₂ PF ₆] ^b	467	681 (principal MLCT emission)	218 ± 3
[[Cu-(3) ₂] ₂ PF ₆] ^b	467	691 (principal MLCT emission)	183 ± 2
[[Cu-(4) ₂] ₂ PF ₆] ^b	467	682 (principal MLCT emission)	178 ± 2
[[Cu-(1) ₂] ₂ PF ₆] ^c	467	690 (principal MLCT emission)	n.a. ^e
[[Cu-(2) ₂] ₂ PF ₆] ^c	467	649 (principal MLCT emission)	n.a. ^e
[[Cu-(3) ₂] ₂ PF ₆] ^c	467	693 (principal MLCT emission)	n.a. ^e
[[Cu-(4) ₂] ₂ PF ₆] ^c	467	663 (principal MLCT emission)	n.a. ^e

^a DMSO solution. ^b DCM solution. ^c Solid state. ^d Uncorrected. ^e n.a. = not applicable.**Fig. 10** Free ligand fluorescence (insets are expansions from 350 to 550 nm for ligands 2 and 4).

Anhydrous 1,10-phenanthroline exhibits structured fluorescence in DCM solution from the lowest-lying singlet state, S₁, with peak maxima at 360, 380 and 400 nm.^{62,63} Phenyl substituents at the 2 and 9 positions are known to bathochromically shift the emission of phenanthroline ligands.⁶² The shift is even more pronounced when electron-donating groups are present on the phenyl substituents, as is the case with ligands 1-4. This is consistent with emission that arises from a π-π* state that is polarized along the transverse axis (as is the case with the ¹L_b excited state^{56,57}). Similar effects have been observed with 3,8-disubstituted phenanthroline ligands.⁶⁴

Room temperature fluid emission is often quenched in the presence of either oxygen-containing or Lewis basic solvents.⁷ Nevertheless, charge-transfer emission has been observed for bis-phenanthroline Cu(I) complexes in solutions of weakly coordinating solvents such as dichloromethane if the copper (I) metal center is sufficiently protected from Lewis base attack through the use of bulky phenanthroline ligands such as when phenyl groups are attached at the 2 and 9 positions.⁸ The Cu(I) complexes in this study were all soluble in DCM, (the solvent used for the ATRA reactions); and room temperature MLCT emission spectra of all complexes were obtained as shown in Fig. 11.

**Fig. 11** a) Solution-state MLCT emission in DCM under argon from [Cu(Ligand)₂]₂PF₆ complexes a) immediately after dissolution and b) after 24 hours.

The [Cu-(1)₂]₂PF₆ and [Cu-(3)₂]₂PF₆ complexes were readily soluble in DCM. After sitting in the glovebox sealed under argon for 24 hours, the absorbance and emission intensity were virtually identical (cf. Figures 11(a) and (b)), indicating essentially no change in solubility over time; see also Electronic Supplementary Information (ESI) (Figures S17 and S18). The MLCT luminescence from [Cu-(2)₂]₂PF₆ and [Cu-(4)₂]₂PF₆ was comparatively weak, initially, in solution due

to the relatively poor solubility of these complexes in DCM. However, after sitting for 24 hours, the solubility of these complexes and consequent emission intensity increased, roughly, by a factor of three (see Figure 11(b)).

The presence of the phenyl groups at the 2 and 9 positions provide protection for the Cu(I) metal center. In 3-D models made from the crystal structure of $[\text{Cu}(\text{3})_2]\text{PF}_6$, significant π -stacking interactions between the phenyl groups and the phenanthroline rings help to stabilize a structure which protects the copper center from attack by either donor solvents or oxygen. Previous studies (involving sterically demanding, non- π -stacking, alkyl substituents at the 2 and 9 positions) indicate that one of the two phenanthroline ligands can be lost and replaced by two solvent molecules with relatively weak donor strength or other ligands due to ligand-ligand interactions.⁶⁵ However, this behavior was not observed in the relatively poor donor solvent DCM in either study. When samples were exposed to air and the emission spectra obtained, no loss of emission intensity (which would be indicative of quenching) was observed (see ESI (Figure S18)). The lifetimes of all four samples (Table 2) are significantly longer than the analogous lifetime for the 2,9-dimethyl analog (90 ns).⁶⁶ Yet the lifetimes are consistent with other 2,9-aryl analogs (e.g., 270 ns for $^*[\text{Cu}(\text{dap})_2]^+$;^{19a} this is, again, indicative of protection of the copper(I) center from donor quenching.

All four complexes display MLCT emission that is broad and red shifted relative to the emission observed from the 2,9-diphenyl analog at 675 nm.⁸ We attribute these characteristics to the electron-donating ability of the hydroxy and methoxy groups to stabilize the excited-state orbitals.⁶⁷ The ability of phenolic moieties to undergo protonation/deprotonation is also well-known to red shift their emission relative to benzenoid species in solution.⁶⁸ The emission spectra of the Cu(I) complexes, in the solid state are shown in Fig. 12.

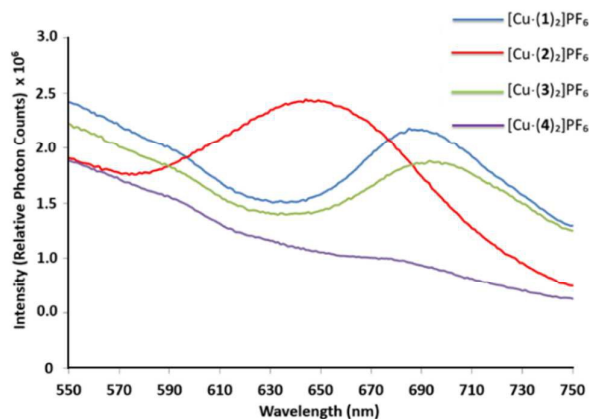


Fig. 12 Solid-state MLCT emission from $[\text{Cu}(\text{Ligand})_2]\text{PF}_6$ complexes.

Unlike the case of the phenyl-substituted analog, the emission in the solid state does not match that in solution.⁶⁹ The emission maxima in the solid state for the complexes

containing the phenol groups, i.e., $[\text{Cu}(\text{2})_2]\text{PF}_6$ and $[\text{Cu}(\text{4})_2]\text{PF}_6$, are blue-shifted relative to the dimethoxy-substituted Cu(I) phenanthroline complexes, i.e., $[\text{Cu}(\text{1})_2]\text{PF}_6$ and $[\text{Cu}(\text{3})_2]\text{PF}_6$, as well as the emission maximum reported for the unsubstituted 2,9-diphenyl phenanthroline analog (675 nm).^{8,67} This is most likely due to the electron-donating effect of the hydroxy group. The effect is somewhat modulated in the case of compound $[\text{Cu}(\text{4})_2]\text{PF}_6$ due to the electron-releasing ability of the added methyl groups. The substantial blue shift of the phenol-substituted phenanthroline, i.e., $[\text{Cu}(\text{2})_2]\text{PF}_6$, in the solid state relative to fluid solution may also be partially due to the ability of the phenol to hydrogen bond in the solid state. Hydrogen bonding may inhibit the ability of the Cu(I) complex to effectively Jahn-Teller distort in the excited state, which may in turn blue shift the emission maxima relative to the other Cu(I) substituted species, where excited state geometric relaxation leads to a lower energy MLCT excited state.

DFT and TDDFT calculations

DFT and TDDFT calculations were performed on all of the free ligands and the cationic moieties of the complexes to further the understanding of the photophysics. Calculations using PW91 and def2-TZV/def2-TZV(p) accurately reproduced the geometric parameters from the solid-state structures. Cu-N bond distances of 2.051 or 2.052 were observed in each of the calculated structures. The NCuN/NCuN interplanar angle was between 70 and 71°, in excellent agreement with the crystal structures. TDDFT was applied in order to elucidate the nature of the electronic transitions observed by UV/vis spectroscopy and utilized for the photocatalytic studies (vide infra). The electronic excitations of the ligands were also calculated and the lowest energy transitions with the highest oscillator strengths are given in Table 3. These all correspond to π - π^* transitions. The lowest energy transition compares well with the experimentally measured absorption (Table 1) when B3PW91 is used (<0.2 eV difference). PW91 gives an underestimation of the energy by ~0.4 eV. It should be noted that solvent effects are not accounted for and may contribute to the observed differences between experimental and calculated values.

Table 3 Three lowest energy transitions in ligands 1-4 by B3PW91

Ligand	λ_1 (nm)	λ_2 (nm)	λ_3 (nm)
1	365	331	324
2	360	327	320
3	369	335	328
4	365	332	324

The calculated electronic excitations of the complexes ($[\text{Cu}(\text{1})_2]^+ - [\text{Cu}(\text{4})_2]^+$) contain transitions that are associated with the ligand π - π^* transitions in the same (as above) energy region. However, there are a number of new transitions that appear at lower energy (Table 4). These new transitions have smaller oscillator strengths (ranging from 0.23–0.45) and are consistent with the expected d- π^* transitions. The lowest energy bands can be arranged in two sets, one originating

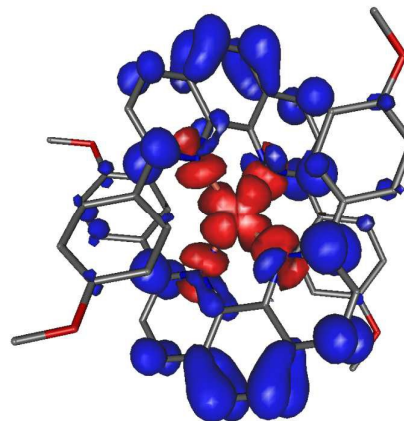
from the HOMO (~570 nm) and one originating from the HOMO-1 (~430 nm), that likely correspond to individual bands in the absorption spectrum.

Table 4 Six lowest energy transitions in complexes $[\text{Cu}(\mathbf{1})_2]^+$ – $[\text{Cu}(\mathbf{4})_2]^+$ by TDDFT

π^*	Band 1 ($d_{\text{HOMO}} \rightarrow \pi^*$)			Band 2 ($d_{\text{HOMO-1}} \rightarrow \pi^*$)		
	L	L+1	L+2	L	L+1	L+2
Complex	λ_1 (nm)	λ_2 (nm)	λ_3 (nm)	λ_4 (nm)	λ_5 (nm)	λ_6 (nm)
$[\text{Cu}(\mathbf{1})_2]^+$	612	551	549	456	430	429
$[\text{Cu}(\mathbf{2})_2]^+$	609	552	543	453	429	423
$[\text{Cu}(\mathbf{3})_2]^+$	624	563	559	458	432.7	431.5
$[\text{Cu}(\mathbf{4})_2]^+$	617	558	549	456	432	426

A distinction should be made between those that populate the LUMO energy levels and those that populate the nearly degenerate LUMO+1 and LUMO+2 levels. The three excitations around 430 nm have the highest oscillator strengths of the two sets and likely correspond to the observed λ_{max} in the $d\text{-}\pi^*$ region of the experimental absorption spectra (~450 nm). Fig. 13 illustrates the charge redistribution upon photoexcitation of $[\text{Cu}(\mathbf{1})_2]^+$ at λ_2 and λ_3 . These transitions correspond best with the 525 nm light source used for excitation (see Photoredox catalysis below). From the charge redistributions in Fig. 13, it is clear that this is formally an oxidation of the metal center and that the copper ion should be treated as Cu^{2+} in such a photoexcited state. Furthermore, the charge is well distributed around the periphery of the phenanthroline rings when it is transferred to the LUMO+1 or LUMO+2, in contrast to being more localized in the interior of the complex when the electron is transferred to the LUMO.

a)



b)

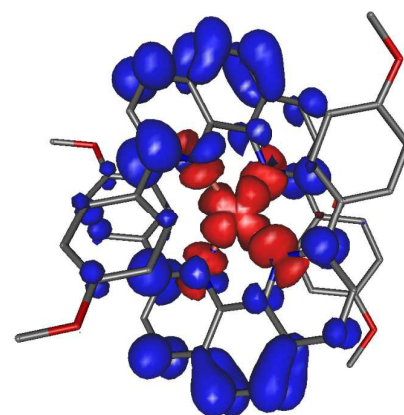


Fig. 13 Transition densities for $d\text{-}\pi^*$ excitations at 551 and 549 nm (a and b, respectively) for complex $[\text{Cu}(\mathbf{1})_2]^+$. Isosurface plotted at 0.001 au. Red and blue represent the depletion and accumulation of electron density upon excitation, respectively. Hydrogen atoms have been removed for clarity.

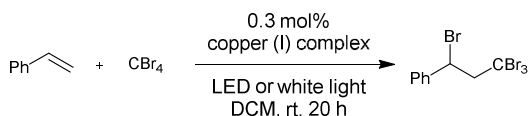
Photoredox catalysis

Photoredox catalysis, initiated by visible-light, is a rapidly developing area of chemical research and it is quickly becoming an attractive tool in organic synthesis.^{19b,20,70} However, most transition metal-based photoredox catalysts, that are capable of utilizing visible-light, incorporate ruthenium or iridium.⁷¹ The high cost, scarcity and toxicity of these metals makes their replacement with earth-abundant elements, like copper and iron, highly desirable. Indeed some of our recent efforts have focused on achieving this goal.⁷² Moreover, a number of successful precedents have demonstrated copper-based complexes to be effective photoredox catalysts.^{19b,20d,73} As such, we hypothesized that, with suitable irradiation from LEDs, $[\text{Cu}(\mathbf{1})_2]\text{PF}_6$ – $[\text{Cu}(\mathbf{4})_2]\text{PF}_6$ might function as photocatalysts in an appropriate photocatalytic reaction cycle.

To probe the viability of these complexes as photocatalysts, the ATRA of CBr_4 to styrene was selected as a test reaction.

Indeed, the closely related complex, i.e., [Cu(dap)₂Cl] (dap = 2,9-bis(*para*-anisyl-1,10-phenanthroline)) was previously demonstrated to be a viable catalyst in such a transformation.^{19b} Thus, the new copper (I) hexafluorophosphate complexes [Cu-(1)₂]PF₆–[Cu-(4)₂]PF₆ were screened for activity as possible photoredox catalysts in this ATRA. The results of this ATRA study are listed in Table 5.

Table 5 Visible light-induced photoredox ATRA reactions



Entry	LED	Copper (I) Complex	Isolated Yield (%) ^a
1	525 nm	[Cu-(1) ₂]PF ₆	91
2	525 nm	[Cu-(2) ₂]PF ₆	36
3	525 nm	[Cu-(3) ₂]PF ₆	95
4	525 nm	[Cu-(4) ₂]PF ₆	56
5	525 nm	[Cu(CH ₃ CN) ₄]PF ₆	N.R.
6	525 nm	[Cu-(2,9-dmp) ₂]PF ₆ ^b	12
7	525 nm	[Cu-(4,7-dpp) ₂]PF ₆ ^c	N.R.
8	525 nm	[Cu-(1) ₂]Cl	91
9	525 nm	[Cu-(1) ₂]BF ₄	96
10	450 nm	[Cu-(1) ₂]PF ₆	79
11	590 nm	[Cu-(1) ₂]PF ₆	N.R.
12	40 W Soft White	[Cu-(1) ₂]PF ₆	49
13 ^d	525 nm	[Cu-(1) ₂]PF ₆	89
14 ^e	525 nm	[Cu-(1) ₂]PF ₆	26
15 ^f	525 nm	[Cu-(1) ₂]PF ₆	6

^a Average of 2 reactions.

^b 2,9-dmp = 2,9-dimethylphenanthroline.

^c 4,7-dpp = 4,7-diphenylphenanthroline.

^d The crude [Cu-(1)₂]PF₆ complex, without purification (no column chromatography; the ¹H NMR spectrum of the crude complex only showed signals for the complex), was used directly in the ATRA reaction. The reaction mixture was prepared (under an Ar atmosphere in a glove box) and sealed, prior to irradiation and stirring.

^e Similar procedure as in footnote d above except that the crude catalyst, without purification, was dissolved in DCM and the reaction mixture was prepared and sealed in an open-air environment, prior to irradiation and stirring.

^f Ligand **1** was dissolved in freshly distilled DCM, and then 0.5 equiv. [Cu(CH₃CN)₄]PF₆ was added to the solution. After stirring 20 min at room temperature, styrene and CBr₄ were added into the solution. The reaction mixture was prepared and sealed in an open-air environment, prior to irradiation and stirring.

Under the semi-optimized reaction conditions (see Experimental Section), the ATRA of CBr₄ to styrene occurs readily to produce (1,3,3,3-tetrabromopropyl)benzene, in a range of yields, at room temperature with low catalyst loadings (0.3 mol%). With LED irradiation (525 nm, green light)

both complexes [Cu-(1)₂]PF₆ and [Cu-(3)₂]PF₆ afforded excellent yields of the corresponding ATRA product (Table 5, Entries 1 and 3). In contrast, under identical conditions, complexes [Cu-(2)₂]PF₆ and [Cu-(4)₂]PF₆ provided low to modest yields of the ATRA product (Table 5, Entries 2 and 4). The primary difference between [Cu-(1)₂]PF₆ and [Cu-(3)₂]PF₆ versus [Cu-(2)₂]PF₆ and [Cu-(4)₂]PF₆ is the presence of the methoxy- versus the hydroxy-substituents in the ligand framework. The relative under-performance of [Cu-(2)₂]PF₆ and [Cu-(4)₂]PF₆ as photocatalysts is likely due to the presence of the phenolic moieties in the ligand structures, as phenolic substances are well-known to serve as inhibitors, in low levels (1.2 mol% in this case), of free radical chain reactions.⁷⁴

We examined the use of a related copper (I) complex, Cu(CH₃CN)₄PF₆, in the absence of any phenanthroline ligand (Table 5, Entry 5). In this case, no ATRA product was observed. This suggests that the presence of the phenanthroline ligand is, indeed, vital to the operation of the ATRA mechanism. To further probe this hypothesis, copper (I) hexafluorophosphate complexes of phenanthroline ligands that possess either smaller 2,9-substituents or varied positioning of bulky diaryl substituents were employed. Specifically, when 0.3 mol% of bis(2,9-dimethylphenanthroline)copper (I) hexafluorophosphate was tested in the ATRA (Table 5, Entry 6), under otherwise identical conditions to the above trials, only 12% of the ATRA product was isolated. Additionally, when 0.3 mol% of bis(4,7-diphenylphenanthroline)copper (I) hexafluorophosphate was tested (Table 5, Entry 7), again under the same reaction conditions, no ATRA product was observed.

We were further interested in examining the role that the counter anion may play in this reaction.^{66,73b} It has been demonstrated that, at sufficiently high concentrations, the counter anion can participate in exciplex quenching of the Jahn-Teller distorted excited-state complex and thereby reduce the lifetime of the catalytically-active excited state.⁷⁵ This effect has been shown to be more pronounced with more nucleophilic anions. Hence, we screened complexes [Cu-(1)₂]Cl^{19b} and [Cu-(1)₂]BF₄ (Table 5, Entries 8 and 9) and found little-to-no change in the product yields compared to the best comparable results (Table 5, Entries 1 and 3). Thus, although it may be anticipated that the chloride anion might bind to the cationic copper center within such a complex and possibly inhibit the reaction, no such deactivation was observed. This experiment and those above suggest that the copper (I) center, within either complex, [Cu-(1)₂]PF₆ and [Cu-(3)₂]PF₆, is sterically shielded by the bulky 2,9-diaryl substituents on the phenanthroline ligands and thus inaccessible to directly bind even a single chloride anion, let alone the reactants as in a Lewis acid-catalyzed mechanism. This is also consistent with the significantly less pronounced exciplex quenching observed with copper(I) bis(2,9-diphenyl-1,10-phenanthroline) as compared with the less sterically crowded copper(I) bis(2,9-dimethyl-1,10-phenanthroline) by various counter anions.⁷⁵ There is, however, still the possibility

that the reaction proceeds more quickly with the less nucleophilic anions, but that, after 20 h, the reaction proceeds to completion so the difference cannot be discerned.

The effects of use of different wavelengths of light on the reaction yield were also probed. Given that the observed λ_{max} for the $^1\text{MLCT}$ occurs at ~ 450 nm, $[\text{Cu}(\cdot\text{1})_2]\text{PF}_6$ was submitted to modified reaction conditions (LED = 450 nm, blue light; Table 5, Entry 10) that sought to match the excitation and absorption wavelengths. Surprisingly, this resulted in a moderate decrease in the isolated yield of the ATRA product, i.e., from 91% to 79%, despite a better energetic match and a higher photon flux (see relative energies of the LED sources in Fig. S16).

In an attempt to resolve this apparent discrepancy, a light source (that was anticipated to excite only the HOMO-LUMO transition) was used. Notably, under these conditions (LED = 590 nm, amber light; Table 5, Entry 11), $[\text{Cu}(\cdot\text{1})_2]\text{PF}_6$ proved to be catalytically unviable. According to the DFT calculations, this transition populates the LUMO (Table 1 and Fig. 14). This indicates that the electron that is transferred to the LUMO is unable to reduce CBr_4 , likely for one of, or some combination of the following reasons: 1) outer sphere electron transfer to the CBr_4 is inefficient because the charge is localized on the interior of the molecule, 2) the LUMO, or more specifically the resulting triplet, is not sufficiently reducing, or 3) the lifetime of the MLCT state that populates the LUMO is too short to allow for efficient electron transfer to CBr_4 .

Given this, it becomes possible to rationalize the poorer performance of the higher energy (450 nm) light source. Given that the DFT-calculated excitation (that overlays best with the 450 nm excitation) also populates the LUMO, a portion of the emitted light will activate a transition that results in catalytically-inactive excited state species. The observed activity that does occur upon irradiation with the 450 nm source likely only results from the more modest overlap with the excitations centred at 551, 549, 432 and 426 nm (Table 4) that populate the LUMO+1 and LUMO+2 as illustrated in Fig. 14. In contrast to the LUMO, these orbitals are higher in energy and therefore more reducing, would have charge localized on the periphery of the molecule and must have a sufficient lifetime to allow the reaction to take place efficiently.

A common 40 W soft white light bulb was also tested in this reaction (Table 5, Entry 12). In this case, a lower yield (49%) of the product was again observed. Thus, the wavelength of the LED/light, or more specifically, the ligand orbital that is populated upon excitation is indeed critical in the reaction.

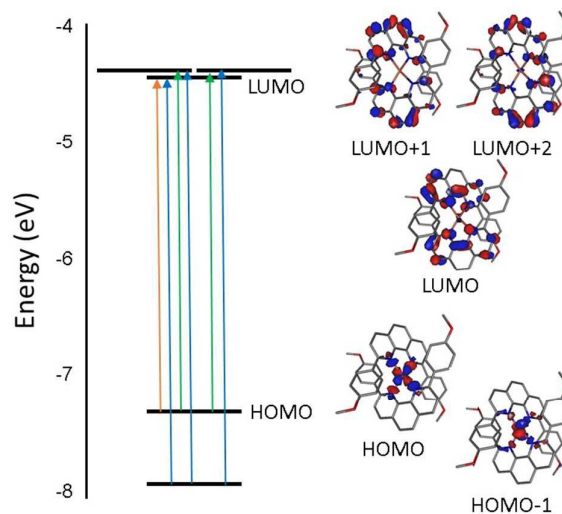
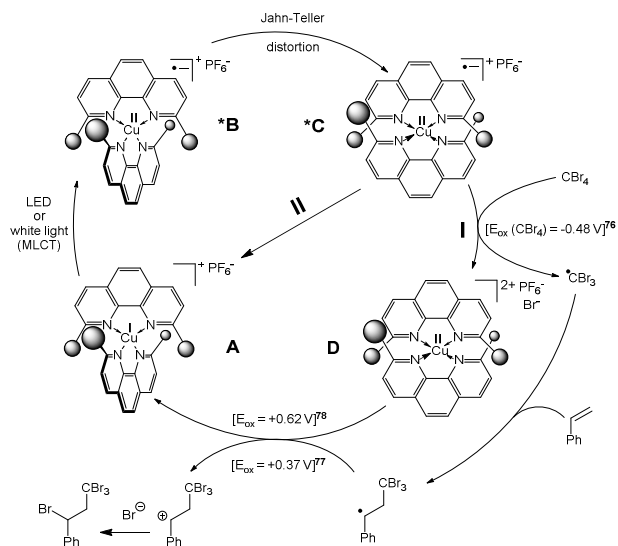


Fig. 14 MO diagram for $[\text{Cu}(\cdot\text{1})_2]^+$ with the six lowest energy transitions shown with arrows. The arrow color represents the color of the LED (amber = 590 nm, green = 525 nm, blue = 450 nm) that corresponds to the energy of the transition. Relevant orbital diagrams are provided plotted at isosurface values of 0.04 au.

Finally, we explored the use of relatively simplified reaction procedures to more easily carry-out this ATRA chemistry. We probed the use of crude catalyst, thereby eschewing the need for chromatographic purification of the catalyst and we were contented to find only a small decrease in the reaction yield (Table 5, Entry 13). Lastly, we attempted to create an all-bench-top protocol in which the reaction components were added (sequentially) under air (Table 5, Entries 14 and 15). In both cases a precipitous drop in the reaction yields were observed (26 and 6%, respectively), underscoring the essential need for inert-atmosphere techniques to successfully facilitate this ATRA chemistry.

Mechanism of photoredox catalysis

A proposed mechanism for the copper (I)-catalyzed photoredox ATRA reaction is shown in Scheme 5 (adapted from reference 19b). Suitable irradiation of the reaction mixture causes photoexcitation of complex **A** via metal-to-ligand charge transfer (MLCT).^{73b,79} This photo-induced charge separation thus leads to an excited state complex (***B**) wherein the copper center is oxidized from (I) to (II) while a complexed phenanthroline ligand is reduced to a radical anion (nevertheless, the overall complex charge is unchanged, i.e., +1).^{66,79,80} As the copper (II) metal center in ***B** is Jahn-Teller active, the complex undergoes tetragonal distortion from a pseudo-tetrahedral geometry (***B**) to a pseudo-square planar geometry (***C**),^{73b,79,80} in so much as possible with the bulky 2,9-diaryl substituents on the phenanthroline ligands.^{80,81}



Scheme 5 Proposed mechanism of the copper (I) complex-catalyzed, photoredox, ATRA reaction (Pathway I is followed if excitation populates the LUMO+1 or LUMO+2, pathway II is followed if excitation populates the LUMO).

Given this distortion and that the Cu(II) center within the excited state complex (***C**) is coordinatively unsaturated, there is potential for the Cu(II) center to bind an additional ligand (such as anion, substrate or solvent) and become a 5- (or 6-) coordinate exciplex.^{66,81} However, given the significant bulk of the 2,9-diaryl substituents and the poor coordinating nature of the other reaction components (i.e., substrates, solvent), it is unlikely that exciplex forms as such typically results in rapid deactivation via non-operative processes.^{19a,66,82} Rather, due to the sufficiently long life of the excited state complex (***C**), (lifetime = 236 ns for $[\text{Cu}(\text{dap})_2]\text{PF}_6$, vide supra; lifetime = 270 ns for $[\text{Cu}(\text{dap})_2]^+\text{BF}_4$ ^{19a,20c}), and the strong reducing potential of ***C**, excited state complex ***C** may take part in an oxidative quenching cycle when the excitation involves populating the LUMO+1 and/or LUMO+2.^{19a,36a,66}

As ***C** is a strong reductant and sufficiently long-lived, fairly efficient outer sphere electron-transfer occurs from the complexed phenanthroline radical anion to the oxidative quencher, in this case, CBr_4 ($E_{\text{ox}} = -0.48 \text{ V}$),⁷⁶ except when the electron of the radical ion is populating the LUMO. This results in cleavage of one of the carbon-bromine bonds of CBr_4 and thus forms the tribromomethyl radical and a bromide anion as well as the ground state Cu(II) complex **D**. The Cu(II) in **D** is surrounded by the two engaging phenanthroline ligands that provide a tetragonally-distorted pseudo-tetrahedral ligand environment. As this ligand environment is not optimal for the Cu(II) ion (where Cu(II) is more stable in a 5- (or 6-) coordinate ligand environment), complex **D** is strained and reactive. This strain is evidently relieved by reduction of the Cu(II) in **D** back to Cu(I), which thus provides the original Cu(I) complex (**A**), thereby completing the catalytic cycle.

The reduction of the Cu(II) in **D** to Cu(I) in **A** is coupled to the oxidation of the in situ-formed benzylic radical (derived from the regioselective addition of the CBr_3 radical to the pi bond of styrene) to provide the benzylic carbocation. While the Cu(II) complex (**D**) is associated with both the PF_6 and the Br anions, reduction to Cu(I) (**A**) concurrently generates the carbocation in close proximity to the (now) free bromide anion. Rapid capture of the carbocation by the nucleophilic bromide anion (in contrast to the non-nucleophilic PF_6 anion) completes the regioselective addition reaction and thus provides the observed product. It is this final redox couple involving reduction of $\text{Cu}(\text{dap})_2^{2+}$ (i.e., reduction of **D** to **A** coupled to oxidation of the benzylic radical to the benzylic carbocation) that is key to closing the catalytic cycle without the need for addition of an external stoichiometric reductant.^{20d}

Conclusions

We have synthesized several 2,9-di(aryl)-1,10-phenanthroline copper (I) complexes in high yield. The complexes were characterized by ^1H NMR and ^{13}C NMR spectroscopy, HR-MS, and elemental analysis (CHN). The solid-state structures of ligands **1** and **2** and complexes $[\text{Cu}(\text{-1-})_2]\text{PF}_6$ and $[\text{Cu}(\text{-3-})_2]\text{PF}_6$ were determined by single-crystal X-ray analysis. Several of the copper complexes were screened as catalysts in a photoredox ATRA reaction involving the regioselective addition of CBr_4 to styrene. Complexes $[\text{Cu}(\text{-1-})_2]\text{PF}_6$ and $[\text{Cu}(\text{-3-})_2]\text{PF}_6$ were found to be very effective photoredox catalysts for this transformation with a very low catalyst loading (0.3 mol%) and without the need for any additional reaction components such as an initiator or stoichiometric reductant. A combination of experiments and calculations suggest that the strong wavelength dependence of the reaction is a result of the markedly differing abilities of the LUMO vs. LUMO+1/+2 in the excited state complex to facilitate the reduction of the CBr_4 .

Acknowledgements

Financial support from the National Science Foundation (MFM research grant CHE-0847736 and NMR instrument grant CHE-1048553) and the Robert A. Welch Foundation (AFC grant D-1838 and MF grant D-1807) are gratefully acknowledged. We thank Prof. Mechref and Dr. Surowiec for HR-MS data and CHN analysis. We thank Dr. Daniel Unruh for discussions of the X-ray diffraction data. We also thank the Department of Chemistry and Biochemistry of Texas Tech University for use of the instrumental facilities.

Notes and references

‡ Electronic Supplementary Information (ESI):
CCDC 986470-986473 contain the supplementary crystallographic data for this paper. These data can be obtained free of charge from the Cambridge Crystallographic Data Centre via http://www.ccdc.cam.ac.uk/data_request/cif.

ARTICLE

Journal Name

or from the Cambridge Crystallographic Data Centre, 12 Union Road, Cambridge CB2 1EZ, UK; fax: (+44) 1223-336-033; e-mail: deposit@ccdc.cam.ac.uk.

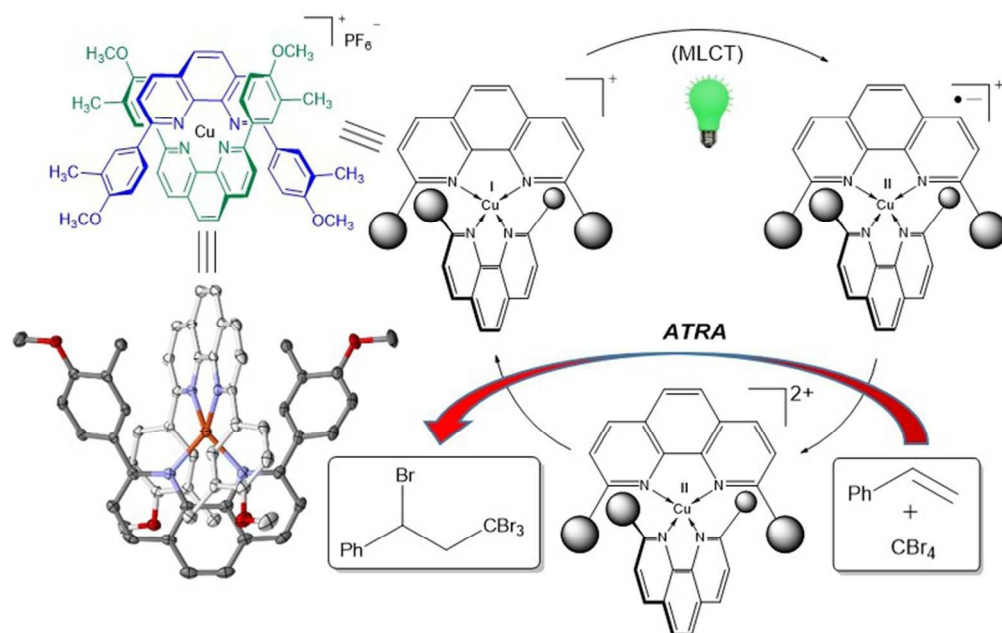
- (a) F. Blau, *Ber.*, 1888, **21**, 1077-1078; (b) Gerdeissen, *Ber.*, 1889, **22**, 244-254; (c) F. Blau, *Monatsh. Chem.*, 1898, **19**, 647-689.
- (a) P. G. Sammes and G. Yahioğlu, *Chem. Soc. Rev.*, 1994, **23**, 327-334; (b) G. Accorsi, A. Listorti, K. Yoosaf and N. Armaroli, *Chem. Soc. Rev.*, 2009, **38**, 1690-1700; (c) S. Sakaki, G. Koga and K. Ohkubo, *Inorg. Chem.*, 1986, **25**, 2330-2333; (d) S. Sakaki, G. Koga, S. Hinokuma, S. Hashimoto and K. Ohkubo, *Inorg. Chem.*, 1987, **26**, 1817-1819; (e) M. T. Buckner, T. G. Matthews, F. E. Lytle and D. R. McMillin, *J. Am. Chem. Soc.*, 1979, **101**, 5846-5848; (f) R. A. Rader, D. R. McMillin, M. T. Buckner, T. G. Matthews, D. J. Casadonte, R. K. Lengel, S. B. Whittaker, L. M. Darmon and F. E. Lytle, *J. Am. Chem. Soc.*, 1981, **103**, 5906-5912; (g) A. A. Del Paggio and D. R. McMillin, *Inorg. Chem.*, 1983, **22**, 691-692; (h) D. J. Casadonte and D. R. McMillin, *Inorg. Chem.*, 1987, **26**, 3950-3952.
- (a) G. Chelucci, A. Saba, G. Sanna and F. Socolini, *Tetrahedron: Asymmetry*, 2000, **11**, 3427-3438; (b) E. Schoffers, *Eur. J. Org. Chem.*, 2003, **7**, 1145-1152.
- L. A. Summers, *Adv. Heterocycl. Chem.*, 1978, **22**, 1-69.
- (a) F. P. Dwyer and D. P. Mellor, *Chelating Agents and Metal Chelates*, Academic Press, New York, 1964; (b) E. D. McKenzie, *Coord. Chem. Rev.*, 1971, **6**, 187-216.
- (a) J.-M. Lehn and A. Rigault, *Angew. Chem., Int. Ed. Engl.*, 1988, **27**, 1095-1097; (b) E. C. Constable, M. G. B. Drew and M. D. Ward, *J. Chem. Soc., Chem. Commun.*, 1987, **20**, 1600-1601; (c) N. Alonso-Vante, V. Ern, P. Chartier, C. O. Dietrich-Buchecker, D. R. McMillin, P. A. Marnot and J.-P. Sauvage, *Nouv. J. Chim.*, 1983, **7**, 3-5.
- M. W. Blaskie and D. R. McMillin, *Inorg. Chem.*, 1980, **19**, 3519-3522.
- C. O. Dietrich-Buchecker, P. A. Marnot, J.-P. Sauvage, J. R. Kirchhoff and D. R. McMillin, *J. Chem. Soc., Chem. Commun.*, **1983**, 513-515.
- (a) L. Bertolo, S. Tamburini, P. A. Vigato, W. Porzio, G. Macchi and F. Meinardi, *Eur. J. Inorg. Chem.*, **2006**, 2370-2376; (b) S. Park, C. D. Sunesh, H. Kim, H. Chae, J. Lee and Y. Choe, *Surf. Interface Anal.*, **2012**, **44**, 1479-1482; (c) M. Chandran, Y. Kwon and Y. Choe, *Mol. Cryst. Liq. Cryst.*, **2014**, **601**, 173-181.
- (a) F. G. Gao and A. J. Bard, *Chem. Mater.*, **2002**, **14**, 3465-3470; (b) H. Tang, Y. Li, Q. Chen, B. Chen, Q. Qiao, W. Yang, H. Wu and Y. Cao, *Dyes Pigment.*, **2014**, **100**, 79-86.
- (a) C. L. Linfoot, P. Richardson, T. E. Hewat, O. Moudam, M. M. Forde, A. Collins, F. White and N. Robertson, *Dalton Trans.*, 2010, **39**, 8945-8956; (b) Q. Zhang, Q. Zhou, Y. Cheng, L. Wang, D. Ma, X. Jing and F. Wang, *Adv. Mater.*, 2004, **16**, 432-436; (c) Q. Zhang, Q. Zhou, Y. Cheng, L. Wang, D. Ma, X. Jing and F. Wang, *Adv. Funct. Mater.*, 2006, **16**, 1203-1208; (d) T. McCormick, W.-L. Jia and S. Wang, *Inorg. Chem.*, 2006, **45**, 147-155; (e) H. Ge, W. Wei, P. Shuai, G. Lei and S. Qing, *J. Lumin.*, 2011, **131**, 238-243; (f) R. S. Khnayzer, C. E. McCusker, B. S. Olaiya and F. N. Castellano, *J. Am. Chem. Soc.*, 2013, **135**, 14068-14070.
- N. Armaroli, G. Accorsi, M. Holler, O. Moudam, J.-F. Nierengarten, Z. Zhou, R. T. Wegh and R. Welter, *Adv. Mater.*, 2006, **18**, 1313-1316.
- (a) R.-S. Lin, M.-R. Li, Y.-H. Liu, S.-M. Peng and S.-T. Liu, *Inorg. Chim. Acta*, 2010, **363**, 3523-3529; (b) K. S. Yoo, C. H. Yoon and K. W. Jung, *J. Am. Chem. Soc.*, 2006, **128**, 16384-16393.
- (a) C. Jallabert, C. Lapinte and H. Riviere, *J. Mol. Catal.*, 1982, **14**, 75-86; (b) C. Jallabert and H. Riviere, *Tetrahedron Lett.*, 1977, 1215-1218; (c) A. M. Sakharov and I. P. Skibida, *J. Mol. Catal.*, 1988, **48**, 157-174; (d) H. Korpi, P. J. Pawel, E. Lankinen, P. Ryan, M. Leskela and T. Repo, *Eur. J. Inorg. Chem.*, 2007, 2465-2471.
- (a) D. Tzalis and P. Knochel, *Tetrahedron Lett.*, 1999, **40**, 3685-3688; (b) W. Cabri and I. Candiani, *Acc. Chem. Res.*, 1995, **28**, 2-7; (c) K. Soai, T. Hayasaka and S. Ugajin, *J. Chem. Soc., Chem. Commun.*, 1989, **8**, 516-517.
- (a) I. E. Markó, P. R. Giles, M. Tsukazaki, I. Chellé-Regnaut, A. Gautier, S. M. Brown and C. J. Urch, *J. Org. Chem.*, 1999, **64**, 2433-2439; (b) M. V. Nandakumar, S. Ghosh and C. Schneider, *Eur. J. Org. Chem.*, 2009, 6393-6398.
- (a) W.-H. Sun, S. Zhang, S. Jie, W. Zhang, Y. Li, H. Ma, J. Chen, K. Wedeking and R. Fröhlich, *J. Organomet. Chem.*, 2006, **691**, 4196-4203; (b) M. Zhang, W. Zhang, T. Xiao, J.-F. Xiang and W.-H. Sun, *J. Mol. Catal. A: Chem.*, 2010, **320**, 92-96.
- V. N. Demidov, S. A. Simanova, A. I. Savinov and T. B. Pakhomov, *Russ. J. Gen. Chem.*, 2009, **79**, 2807-2814.
- (a) J.-M. Kern and J.-P. Sauvage, *J. Chem. Soc., Chem. Commun.*, 1987, 546-548; (b) M. Pirtsch, S. Paria, T. Matsuno, H. Isobe and O. Reiser, *Chem. Eur. J.*, 2012, **18**, 7336-7340.
- (a) Q. Yang, F. Dumur, F. Morlet-Savary, J. Poly and J. Lalevee, *Macromolecules*, 2015, **48**, 1972-1980; (b) G. Ferraudi and S. Muralidharan, *Coord. Chem. Rev.*, 1981, **36**, 45-88; (c) A. C. Hernandez-Perez and S. K. Collins, *Acc. Chem. Res.*, 2016, **49**, 1557-1565; (d) O. Reiser, *Acc. Chem. Res.*, 2016, **49**, 1990-1996; (e) S. K. Pagire, S. Paria and O. Reiser, *Org. Lett.*, 2016, **18**, 2106-2109; (f) T. P. Nicholls, G. E. Constable, J. C. Robertson, M. G. Gardiner and A. C. Bissemer, *ACS Catal.*, 2016, **6**, 451-457; (g) W. Ma, D. Chen, Y. Ma, L. Wang, C. Zhao and W. Yang, *Polym. Chem.*, 2016, **7**, 4226-4236.
- B.-J. Li and Z.-J. Shi, *Chem. Sci.*, 2011, **2**, 488-493.
- S. Gupta, P. K. Agarwal, M. Saifuddin and B. Kundu, *Tetrahedron Lett.*, 2011, **52**, 5752-5757.
- H. Hachiya, K. Hirano, T. Satoh and M. Miura, *Org. Lett.*, 2011, **13**, 3076-3079.
- Y. Li, M. Wu, W. Liu, Z. Yi and J. Zhang, *Catal. Lett.*, 2008, **123**, 123-128.
- (a) S. Paria, M. Pirtsch, V. Kais and O. Reiser, *Synthesis*, 2013, **45**, 2689-2698; (b) M. S. Kharasch, E. V. Jensen and W. H. Urry, *Science*, 1945, **102**, 128-128; (c) D. P. Curran, *Synthesis*, 1988, 489-513; (d) D. P. Curran, *Synthesis*, 1988, 417-439; (e) W. T. Eckenhoff and T. Pintauer, *Polymer Preprints*, 2008, **49**, 213-214; (f) M. S. Kharasch, H. Engelmann and F. R. Mayo, *J. Org. Chem.*, 1937, **2**, 288-302.
- (a) W. T. Eckenhoff and T. Pintauer, *Cat. Rev. -Sci. Eng.*, 2010, **52**, 1-59; (b) M. S. Kharasch, W. H. Urry and E. V. Jensen, *J. Am. Chem. Soc.*, 1945, **67**, 1626-1626.
- M. S. Kharasch, P. S. Skell and P. Fisher, *J. Am. Chem. Soc.*, 1948, **70**, 1055-1059.
- (a) H. Yorimitsu, T. Nakamura, H. Shinokubo, K. Oshima, K. Omoto and H. Fujimoto, *J. Am. Chem. Soc.*, 2000, **122**, 11041-11047; (b) H. Yorimitsu, H. Shinokubo, S. Matsubara, K. Oshima, K. Omoto and H. Fujimoto, *J. Org. Chem.*, 2001, **66**, 7776-7785.

- 29 P. Balczewski, A. Szadowiak and T. Bialas, *Heteroat. Chem.*, 2005, **16**, 246-253.
- 30 (a) D. P. Curran, E. Bosch, J. Kaplan and M. Newcomb, *J. Org. Chem.*, 1989, **54**, 1826-1831; (b) D. P. Curran and C.-T. Chang, *J. Org. Chem.*, 1989, **54**, 3140-3157; (c) D. P. Curran, M.-H. Chen, E. Spletzer, C. M. Seong and C.-T. Chang, *J. Am. Chem. Soc.*, 1989, **111**, 8872-8878; (d) D. P. Curran and C. M. Seong, *J. Am. Chem. Soc.*, 1990, **112**, 9401-9403; (e) D. P. Curran and J. Tamine, *J. Org. Chem.*, 1991, **56**, 2746-2750; (f) D. P. Curran and D. Kim, *Tetrahedron*, 1991, **47**, 6171-6188.
- 31 D. Ravelli and M. Fagnoni, *ChemCatChem*, 2015, **7**, 735-737.
- 32 A. J. Clark, *Chem. Soc. Rev.*, 2002, **31**, 1-11.
- 33 M. Kameyama, N. Kamigata and M. Kobayashi, *J. Org. Chem.*, 1987, **52**, 3312-3316; and references therein.
- 34 L. Forti, F. Ghelfi, E. Libertini, U. M. Pagnoni and E. Soragni, *Tetrahedron*, 1997, **53**, 17761-17768.
- 35 R. A. Gossage, L. A. Van De Kuil and G. Van Koten, *Acc. Chem. Res.*, 1998, **31**, 423-431.
- 36 (a) C. K. Prier, D. A. Rankic and D. W. C. MacMillan, *Chem. Rev.*, 2013, **113**, 5322-5363; (b) J. M. R. Narayanam and C. R. Stephenson, *Chem. Soc. Rev.*, 2011, **40**, 102-113; (c) T. P. Yoon, M. A. Ischay and J. Du, *Nat. Chem.*, 2010, **2**, 527-532; (d) K. Zeitler, *Angew. Chem., Int. Ed.*, 2009, **48**, 9785-9789.
- 37 (a) J. D. Nguyen, J. W. Tucker, M. D. Konieczynska and C. R. J. Stephenson, *J. Am. Chem. Soc.*, 2011, **133**, 4160-4163; (b) C.-J. Wallentin, J. D. Nguyen, P. Finkbeiner and C. R. J. Stephenson, *J. Am. Chem. Soc.*, 2012, **134**, 8875-8884.
- 38 (a) Y. Zheng, T. Zhao, B. Newland, J. Poly and W. Wang, *Chem. Commun.*, 2013, **49**, 10124-10126; (b) W. T. Eckenhoff and T. Pintauer, *Inorg. Chem.*, 2010, **49**, 10617-10626; (c) W. T. Eckenhoff and T. Pintauer, *Dalton Trans.*, 2011, **40**, 4909-4917; (d) T. Pintauer, *Eur. J. Inorg. Chem.*, 2010, 2449-2460.
- 39 C. Dietrich-Buchecker and J.-P. Sauvage, *Tetrahedron*, 1990, **46**, 503-512.
- 40 (a) W. Zhong, Y. Tang, G. Zampella, X. Wang, X. Yang, B. Hu, J. Wang, Z. Xiao, Z. Wei, H. Chen, L. De Gioia and X. Liu, *Inorg. Chem. Commun.*, 2010, **13**, 1089-1092; (b) S. Kang, M. M. Cetin, R. Jiang, E. S. Clevenger and M. F. Mayer, *J. Am. Chem. Soc.*, 2014, **136**, 12588-12591.
- 41 G. M. Sheldrick, *SADABS v2008/1*, 2008.
- 42 *CrystalClear-SM Expert v2.0*. Rigaku Americas, The Woodlands, Texas, USA, and Rigaku Corporation, Tokyo, Japan, 2010.
- 43 G. M. Sheldrick, *Acta Crystallogr. Sect. A*, 2008, **64**, 112-122.
- 44 A. L. Spek, *Acta Crystallogr. Sect. D-Biol. Cryst.*, 2009, **65**, 148-155.
- 45 F. Neese, *Wiley Interdiscip. Rev. Comput. Mol. Sci.*, 2012, **2**, 73-78.
- 46 J. P. Perdew and Y. Wang, *Phys. Rev. B*, 1992, **45**, 13244-13249.
- 47 A. Schäfer, H. Horn and R. Ahlrichs, *J. Chem. Phys.*, 1992, **97**, 2571-2577.
- 48 F. Weigend and R. Ahlrichs, *Phys. Chem. Chem. Phys.*, 2005, **7**, 3297-3305.
- 49 F. Neese, *J. Comput. Chem.*, 2003, **24**, 1740-1747.
- 50 A. D. Becke, *Phys. Rev. A*, 1988, **38**, 3098-3100.
- 51 J. E. Beves, B. A. Blight, C. J. Campbell, D. A. Leigh and R. T. McBurney, *Angew. Chem. Int. Ed.*, 2011, **50**, 9260-9327; and references therein.
- 52 M. Nishio, Y. Umezawa, K. Honda, S. Tsuboyama and H. Suezawa, *CrystEngComm*, 2009, **11**, 1757-1788.
- 53 M. Nishio, *CrystEngComm*, 2004, **6**, 130-158.
- 54 R. J. Platt, *J. Chem. Phys.*, 1949, **17**, 484-495.
- 55 R. G. Bray, J. Ferguson and C. J. Hawkins, *Aust. J. Chem.*, 1969, **22**, 2091-2103.
- 56 T. Hoshi, H. Inoue, J. Yoshino, T. Masamoto and Y. Tanizaki, *Z. Phys. Chem. Neue Fol.*, 1972, **81**, 23-30.
- 57 S. F. Mason, *Inorg. Chim. Acta Rev.*, 1968, **2**, 89-109.
- 58 P. Day and N. Sanders, *J. Chem. Soc. A*, 1967, 1530-1536.
- 59 C. C. Deb, D. K. Hazra and S. C. Lahiri, *Indian J. Chem., Sect. A*, 1982, **21**, 26-30.
- 60 C. C. Phifer and D. R. McMillin, *Inorg. Chem.*, 1986, **25**, 1329-1333.
- 61 A. K. I. Gushurst, D. R. McMillin, C. O. Dietrich-Buchecker and J.-P. Sauvage, *Inorg. Chem.*, 1989, **28**, 4070-4072.
- 62 N. Armaroli, L. De Cola, V. Balzani, J.-P. Sauvage, C. O. Dietrich-Buchecker and J.-M. Kern, *J. Chem. Soc., Faraday Trans.*, 1992, **88**, 553-556.
- 63 M. S. Henry and M. Z. Hoffman, *J. Phys. Chem.*, 1979, **83**, 618-625.
- 64 H. S. Joshi, R. Jamshidi and Y. Tor, *Angew. Chem. Int. Ed.*, 1999, **38**, 2722-2725.
- 65 (a) O. Green, B. Ghandi and J. Burstyn, *Inorg. Chem.*, 2009, **48**, 5704-5714; (b) M. K. Eggleston, D. R. McMillin, K. S. Koenig and A. J. Pallenberg, *Inorg. Chem.*, 1997, **36**, 172-176.
- 66 D. R. McMillin, J. R. Kirchoff and K. V. Goodwin, *Coord. Chem. Rev.*, 1985, **64**, 83-92.
- 67 G. Blasse, P. A. Breddels and D. R. McMillin, *Chem. Phys. Lett.*, 1984, **109**, 24-26.
- 68 R. T. Williams and J. W. Bridges, *J. Clin. Pathol.*, 1964, **17**, 371-394.
- 69 E. J. Padma Malar and K. Jug, *J. Phys. Chem.*, 1984, **88**, 3508-3516.
- 70 For pioneering examples, see: (a) D. M. Hedstrand, W. H. Kruizinga and R. M. Kellogg, *Tetrahedron Lett.*, 1978, **19**, 1255-1258; (b) C. Pac, M. Ihama, M. Yasuda, Y. Miyauchi and H. Sakurai, *J. Am. Chem. Soc.*, 1981, **103**, 6495-6497; (c) R. Maidan, Z. Goren, J. Y. Becker and I. Willner, *J. Am. Chem. Soc.*, 1984, **106**, 6217-6222; (d) I. Willner, T. Tsfania and Y. Eichen, *J. Org. Chem.*, 1990, **55**, 2656-2662; (e) K. Hironaka, S. Fukuzumi and T. Tanaka, *J. Chem. Soc. Perkin Trans. 2*, 1984, **10**, 1705-1709.
- 71 For recent examples, see: (a) P. Kohls, D. Yadav, G. Pandey and O. Reiser, *Org. Lett.*, 2012, **14**, 672-675; (b) A. McNally, C. K. Prier and D. W. C. MacMillan, *Science*, 2011, **334**, 1114-1117; (c) M. Rueping, D. Leonori and T. Poisson, *Chem. Commun.*, 2011, **47**, 9615-9617; (d) T. Maji, A. Karmakar and O. Reiser, *J. Org. Chem.*, 2011, **76**, 736-739; (e) A. G. Condie, J. C. González-Gómez and C. R. J. Stephenson, *J. Am. Chem. Soc.*, 2010, **132**, 1464-1465; (f) J. W. Tucker, J. M. R. Narayanam, S. W. Krabbe and C. R. J. Stephenson, *Org. Lett.*, 2010, **12**, 368-371; (g) J. Du and T. P. Yoon, *J. Am. Chem. Soc.*, 2009, **131**, 14604-14606; (h) M. A. Ischay, M. E. Anzovino, J. Du and T. P. Yoon, *J. Am. Chem. Soc.*, 2008, **130**, 12886-12887; (i) T. Koike and M. Akita, *Chem. Lett.*, 2009, **38**, 166-167; (j) X. Sun and S. Yu, *Synlett*, 2016, **27**, 2659-2675.
- 72 (a) F. S. Wekesa, R. Arias-Ugarte, L. Kong, Z. Sumner, G. P. McGovern and M. Findlater, *Organometallics*, 2015, **34**, 5051-5056; (b) A. D. Smith, A. Saini, L. M. Singer, N. Phadke and M. Findlater, *Polyhedron*, 2016, **114**, 286-291; (c) M. D. Redlich, M. F. Mayer and M. M. Hossain, *Aldrichimica Acta*, 2003, **36**, 3-13.

ARTICLE

Journal Name

- 73 (a) O. Horvath, *Coord. Chem. Rev.*, 1994, **135/136**, 303-324; (b) N. Armadori, G. Accorsi, F. Cardinali and A. Listorti, *Top. Curr. Chem.*, 2007, **280**, 69-115.
- 74 (a) P. Alov, I. Tsakovska and I. Pajeva, *Curr. Top. Med. Chem.*, 2015, **15**, 85-104; (b) M. Lucarini and G. F. Pedulli, *Chem. Soc. Rev.*, 2010, **39**, 2106-2119; (c) E. T. Denisov and V. V. Azatyan, *Inhibition of Chain Reactions*; Institute of Problems of Chemical Physics University Press: London, 2000.
- 75 R. M. Everly and D. R. McMillin, *J. Photochem. Photobiol.*, 1989, **50**, 711-716.
- 76 A. A. Isse, C. Y. Lin, M. L. Coote and A. Gennaro, *J. Phys. Chem. B*, 2011, **115**, 678-684.
- 77 D. D. M. Wayner and A. Houmam, *Acta Chem. Scand.*, 1998, **52**, 377-384.
- 78 C. O. Dietrich-Buchecker, J.-P. Sauvage and J.-M. Kern, *J. Am. Chem. Soc.*, 1989, **111**, 7791-7800.
- 79 M. Iwamura, S. Takeuchi and T. Tahara, *J. Am. Chem. Soc.*, 2007, **129**, 5248-5256.
- 80 A. Masood, D. J. Hodgson and P. S. Zacharias, *Inorg. Chim. Acta*, 1994, **221**, 99-108.
- 81 D. R. McMillin and K. M. McNett, *Chem. Rev.*, 1998, **98**, 1201-1219.
- 82 A. K. Ichinaga, J. R. Kirchoff, D. R. McMillin, C. O. Dietrich-Buchecker, P. A. Marnot and J.-P. Sauvage, *Inorg. Chem.*, 1987, **26**, 4290-4292.



136x85mm (150 x 150 DPI)